RAND

Mutual Interference in Fast-Frequency-Hopped, Multiple-Frequency-Shift-Keyed, Spread-Spectrum Communication Satellite Systems

Edward Bedrosian

Project AIR FORCE
Arroyo Center

DTIC QUALITY INSPECTED 3

DISTRIBUTION STATEMENT A
Approved for public release;
Distribution Unlimited

19960917 028

The research described in this report was sponsored jointly by the United States Air Force, Contract F49620-91-C-0003 and by the United States Army, Contract No. MDA903-91-C-0006.

Library of Congress Cataloging in Publication Data

Bedrosian, Edward.
Mutual interference in fast-frequency-hopped, multiple-frequency-shift-keyed, spread-spectrum communication satellite systems / Edward Bedrosian.
p. cm
"Project AIR FORCE."
"Arroyo Center."
"Prepared for the United States Air Force and the United States Army."
"MR-672-AF/A."
Includes bibliographical references.
ISBN 0-8330-2393-4 (alk. paper)
1. Military telecommunication—Computer simulation. 2. Artificial satellites in telecommunication—Computer simulation. 3. Radio-Interference—Computer simulation. 4. Spread spectrum communications. 5. United States—Armed Forces—Communication systems. I. United States. Air Force. II. United States. Army. III. Project AIR FORCE (U.S.). IV. Title.
UG593.B4324 1996
355.8´5´0973—dc20 96-19534
CIP

© Copyright 1996 RAND

All rights reserved. No part of this book may be reproduced in any form by any electronic or mechanical means (including photocopying, recording, or information storage and retrieval) without permission in writing from RAND.

RAND is a nonprofit institution that helps improve public policy through research and analysis. RAND's publications do not necessarily reflect the opinions or policies of its research sponsors.

Published 1996 by RAND
1700 Main Street, P.O. Box 2138, Santa Monica, CA 90407-2138
RAND URL: http://www.rand.org/
To order RAND documents or to obtain additional information, contact Distribution Services: Telephone: (310) 451-7002; Fax: (310) 451-6915; Internet: order@rand.org

RAND

Mutual Interference in Fast-Frequency-Hopped, Multiple-Frequency-Shift-Keyed, Spread-Spectrum Communication Satellite Systems

Edward Bedrosian

Prepared for the
United States Air Force
United States Army

Project AIR FORCE
Arroyo Center

Approved for public release; distribution unlimited

PREFACE

The command and control of modern military forces is becoming increasingly dependent on space assets for a wide variety of functions. Prominent among these are communication satellites, the value of which has been amply demonstrated in recent military operations, notably Operations Desert Shield/Storm. Unfortunately, modern communication satellite systems are very expensive. Given the shrinking military budget and the volatile geopolitical world in which they must be used, it becomes essential to obtain those systems that best serve these uncertain needs and to do so at the least cost.

As part of its research for the Army and the Air Force, RAND is constructing a concept-level modeling tool that is intended to permit evaluating conceptual military communication satellite systems at a systems level. That is, it considers only basic design parameters. This report is the third in a series devoted to presenting the analytical procedures required in such a computer model and does not discuss the model's implementation. The first in the series is MR-639-AF/A, *Concept-Level Analytical Procedures for Loading Nonprocessing Communication Satellites with Nonantijam Signals*, by Edward Bedrosian and Gaylord K. Huth, 1996. The second is MR-640-AF/A, *Concept-Level Analytical Procedures for Loading Nonprocessing Communication Satellites with Direct-Sequence, Spread-Spectrum Signals*, by Edward Bedrosian and Gaylord K. Huth, 1996. A detailed description of the concept-level modeling tool and examples of its use will be presented in a forthcoming report.

This analysis has been conducted jointly under two of RAND's federally funded research and development centers (FFRDCs)—Project AIR FORCE and the Arroyo Center.

Project AIR FORCE is the FFRDC operated by RAND for the U.S. Air Force. It is the only Air Force FFRDC charged with policy analysis. Its chief mission is to conduct objective and independent research and analysis on enduring issues of policy, management, technology, and resource allocation that will be of concern to the senior leaders and decisionmakers of the Air Force. Project AIR FORCE work is performed under contract F49620-91-C-0003. The research reported in this document was conducted under the C4I/Space Project within the Force Modernization and Employment Program of Project AIR FORCE.

The Arroyo Center is a studies and analysis FFRDC operated by RAND for the U.S. Army. It provides the Army with objective, independent analytic research on major

policy and organizational concerns, emphasizing mid- and long-term problems. Arroyo Center work is performed under contract MDA903-91-C-0006. The research reported in this document was conducted under the C3I/Space for Contingency Operations Project within the Force Development and Technology Program of the Arroyo Center.

CONTENTS

Preface iii

Figures vii

Summary ix

Acknowledgments xi

Symbols and Acronyms xiii

Chapter One
INTRODUCTION 1

Chapter Two
FREQUENCY-HOPPED, MULTIPLE-FREQUENCY-SHIFT-KEYED, SPREAD-SPECTRUM SIGNALS 5

Chapter Three
THE HOPPED-SIGNAL ENVIRONMENT IN THE SPREAD BAND 11

Chapter Four
THE MFSK DEMODULATOR 13

Chapter Five
THE SYMBOL ERROR PROBABILITY 19

Chapter Six
AN ANALYTICAL MODEL FOR USER INTERFERENCE 25

Chapter Seven
ANALYSIS OF THE NON-DIVERSITY CASE (N = 1) 31

Chapter Eight
ANALYSIS OF THE DUAL-DIVERSITY CASE (N = 2) 35

Chapter Nine
AN ASYMPTOTIC MODEL FOR THE HIGH-ORDER-DIVERSITY CASE (N >> 1) 39
The Linear Detector 39
The Square-Law Detector 42

Chapter Ten
ANALYSIS OF THE HIGH-ORDER-DIVERSITY CASE (N >> 1) 45

Appendix
A. Quadrature Detector Output 49
B. The Probability Density of a Normalized Rayleigh Variable in dB 51
C. Derivation of the Symbol Error Probability for the Non-Diversity Case 57
D. Derivation of the Density Function of the Sum of the Squares of Two Identically Distributed Independent Ricean Random Variables 61
E. Derivation of the Symbol Error Probability for the High-Order Diversity Case 65
REFERENCES 67

FIGURES

2.1. Basic MFSK System Block Diagram 5
2.2. Frequency-Time Diagram of a Typical MFSK Chip Sequence for M = 8 with Minimum Chip Spacing in Frequency 6
2.3. Basic FH MFSK System Block Diagram 7
2.4. Frequency-Time Diagram of the FH MFSK Chip Sequence Shown in Figure 2.2 for M = 8 7
2.5. Frequency-Time Diagram of the FFH MFSK Chip Sequence Shown in Figure 2.2 for M = 8 and N = 2 8
4.1. Typical Fast-Frequency-Hopping MFSK Demodulator 14
6.1. Probability Density Function of Normalized Rayleigh Variable 27
6.2. Probability Density Function of E_b/I_0 dB for a Terrestrial CDMA Cellular System Employing Power Control 27
6.3. Probability Density Function of Normalized Rayleigh Variable in dB 28
E.1. Regions of Integration for Symbol Error Probability in the High-Order-Diversity Case 66

SUMMARY

This report presents the results of a theoretical analysis of a frequency-hopping, multiple-frequency-shift-keyed, spread-spectrum communication system using a nonprocessing communication satellite transponder. A large number of users are assumed to be hopping pseudo-randomly about the transponder passband in time synchronization and approximate frequency synchronization. The users are assumed to be free to hop independently with the result that they occasionally interfere with one another. Formulations are presented that permit assessment of the level of mutual interference, thereby facilitating the selection of system parameters that will maximize the communication throughput of the system.

The results presented here are purely theoretical. Numerical calculations will be presented in graphical form in a future report. These will then be used to develop a satellite loading procedure. They will also be extended to apply to hard-limiting satellite transponders and to consider the effects of jamming.

ACKNOWLEDGMENTS

The author gratefully acknowledges the invaluable assistance provided by RAND colleagues Gaylord K. Huth, Phillip M. Feldman, and William Sollfrey. Their cheerful cooperation helped the author through many analytical difficulties that this research posed.

SYMBOLS AND ACRONYMS

a	Typical random amplitude of an input tone
C	Euler's constant: $C = 0.57721\ 56649$
CDMA	Code Division Multiple Access
E	Expectation operator
E_b	Received bit energy
f	Power of the desired user relative to the ensemble of users
f_c	One of the pseudo-randomly chosen carrier frequencies
$f(h_{M,N})$	Probability density function of the output of the second sampler in the Mth (signal-bearing) detection channel at the end of the Nth diversity chip
$f_k(t)$	Input at intermediate frequency to the kth detection channel of the MFSK demodulator
FFH	Fast Frequency Hopping (or Hopped)
FH	Frequency Hopping (or Hopped)
$f(t)$	Total input at intermediate frequency to the MFSK demodulator
$g_{k,j}$	Output of the kth detection channel at the end of the jth diversity chip
h	Natural logarithm of 10: $h = 2.30258\ 5093$
$h_{k,N}$	Output of the second sampler in the kth detection channel at the end of the Nth diversity chip
IF	Intermediate Frequency
I_0	Total interference energy spectral density
k	Number of users in the spread band
K	Number of pseudo-randomly hopped carrier frequencies
m	Number of bits per symbol
M	Number of symbols in MFSK alphabet
MFSK	Multiple Frequency Shift Keying (or Keyed)

n Total number of frequency slots available in the spread band

N Order of diversity ≡ the number of symbol repetitions per bit

p Probability that a given user will occupy a given frequency slot during a given hop

pdf Probability density function

$p(h_{k,N})$ Probability density function of the output of the second sampler in the kth (non-signal-bearing) detection channel at the end of the Nth diversity chip

p_i Probability that a given user will occupy the ith frequency slot during a given hop

$p(r_i)$ Probability of r_i users occupying the ith frequency slot during a given hop

$p(r_1, r_2, \cdots, r_n)$ Probability that there will be r_1 users occupying the first frequency slot, r_2 users occupying the second frequency slot, etc., during a given hop

P Average power of ensemble of users

$P_e^b(M,N)$ Probability of bit error probability in an MFSK sysem using Nth-order diversity

$P_e^s(M,N)$ Probability of symbol error in an MFSK system using Nth-order diversity

$\wp_e^s(M,N)$ The probability of symbol error in an MFSK system using Nth-order diversity for a particular set of interfering tones, $[r_{k,j}]$

r_i The number of users occupying the ith frequency slot during a given hop

R_c Chip (or hop) rate

RF Radio Frequency

$r_{k,j}$ Number of tones present in the kth detection channel during the jth diversity chip

$[r_{k,j}]$ The set of MN numbers of interfering tones present in an MFSK system using Nth-order diversity, where $k = 1,2,\cdots,M$ identifies the detection channel and $j = 1,2,\cdots,N$ identifies the diversity chip

SFH Slow Frequency Hopped

T_b Bit duration

T_c Chip (or hop) duration

θ Typical random phase of an input tone

λ The average number of users occupying a given frequency slot during a given hop

$\pi(g_{k,j})$ Probability density function of the output of the first sampler in the kth (non-signal-bearing) detection channel at the end of the jth diversity chip

ρ Generic for the number of tones input to a detection channel

$\phi(g_{M,j})$ Probability density function of the output of the first sampler in the Mth (signal-bearing) detection channel at the end of the jth diversity chip

ω Typical radian frequency of an input tone

Chapter One

INTRODUCTION

Frequency hopping and direct sequence are the two most common types of spread-spectrum modulation used to combat jamming, i.e., deliberate interference. They do this by spreading the signal energy over a much wider bandwidth than that required to convey the basic information stream. When this is done in a fashion that the jammer cannot duplicate (usually by using pseudo-random sequences appropriately), it is possible to retrieve the desired signal while causing the jamming signal energy to be diluted by the bandwidth spreading factor.

It is apparent that spread-spectrum signaling can equally well be used to accommodate a large number of users simultaneously in a large bandwidth by letting each user regard the set of all other users as the interference with which it must cope. Although systems using frequency-division multiplex can make more efficient use of the channel, they are difficult to adapt to a random-multiple-access mode of operation in which a much larger number of users than the channel can accommodate at a given instant wish to have access to the channel for relatively short periods of time at moments of their own choosing.

Frequency-hopping and direct-sequence systems both form the signal data stream into a sequence of symbols that occur at a rate not much different from the information bit rate. Each symbol denotes one or more information bits that have been processed to include coding, encrypting, etc. The bandwidth required to transmit the symbol stream is characteristic of a given system and constitutes the relatively small bandwidth that is to be spread over the much wider transmission channel.

In frequency-hopping systems, the individual symbols are transmitted, either in their entirety or in segments, as "chips," whose center frequencies are changed chip by chip in a pseudo-random fashion so as to cause the average signal energy to be spread pseudo-randomly over the entire channel. In direct-sequence systems, each symbol has its energy spread pseudo-randomly over the entire channel; hence, the channel appears fully occupied at all times.

The interest here is in the cooperative, multiple-access use of frequency-hopping for military communications via a frequency-translating communication satellite. The analysis presented in this report, which treats the unjammed use of a simple linear transponder (of the type found in commercial communication satellites), is the first step in this process. Its length and complexity led to the decision to publish it separately, with supporting numerical computations to be presented in graphical form in

a future report. Subsequent research will include a treatment of hard-limiting transponders and the jamming of both types of transponders.

The theory of a frequency-hopped (FH), multiple-frequency-shift-keyed (MFSK) spread-spectrum comunication system is described in simple terms in Chapter Two to provide a framework for the analysis to follow. Block diagams are used to show how such signals are generated and detected and time-frequency diagrams are used to illustrate how the signal energy is distributed by such a modulation scheme. In Chapter Three the statistics describing how the signals of a large number of MFSK users are distributed about the spread band by the hopping process are developed. These furnish the basis for quantifying the mutual interference they experience from one another.

The structure of a typical MFSK demodulator is presented in block diagram form in Chapter Four, leading to a mathematical description of how its output is related to its input. The technique of diversity transmission and reception, which is integral to operating in the face of interference, intentional or not, is introduced at this point. In Chapter Five, the general expression for the symbol error probability is derived and presented in both the form of an integral representation and an expansion in terms of increasing complexity. The latter is used to illustrate the various approximations and bounds that are of value in some cases.

An analytical model for the interference caused to one another by the various users as they hop about the spread band is developed in Chapter Six. Experimental evidence is presented suggesting that received user powers can be approximated by a log-normal distribution. It is then shown that if the individual received user powers are expressed as two-dimensional Gaussian variates, the sum of a number of such received signals will have a Rayleigh distribution of amplitudes and that the power of such a composite signal approximates a log-normal distribution. Lacking more experimental evidence, the accuracy of this analytical model cannot be assessed but the approximation appears sufficiently promising to warrant using it as the basis for an analysis of a frequency-hopped MFSK system to arrive at a performance evaluation that can be compared with the performance of actual systems. The alternative would be to use the log-normal distribution directly—an approach that would lead to considerable analytical difficulties.

The non-diversity case ($N = 1$) is analyzed in Chapter Seven, culminating in the development of the density functions characterizing the demodulator outputs in the signal-bearing and non-signal-bearing detection channels. These can then be used in the symbol error probability formulations developed in Chapter Five. The dual-diversity case is analyzed in Chapter Eight, where it is shown that an exact formulation, analogous to the one developed in Chapter Seven for the non-diversity case, does not appear possible. However, a bounded solution for the linear detector, which may prove useful in some circumstances, is presented as an example of an analytical alternative. Analytical solutions suitable for orders of diversity greater than two may not be practical, indicating the need for Monte Carlo simulations to obtain performance results.

An asymptotic model for the detection-channel outputs when operating at high orders of diversity ($N >> 1$) is developed in Chapter Nine for both the linear and the square-law detector. The corresponding formulations for the symbol error probability are presented in Chapter Ten.

Chapter Two

FREQUENCY-HOPPED, MULTIPLE-FREQUENCY-SHIFT-KEYED, SPREAD-SPECTRUM SYSTEMS

A basic MFSK system is shown in block diagram form in Figure 2.1. In the transmitter, the binary information data stream is first processed (e.g., coded for error correction) and then buffered m bits at a time in a binary m-tuple, which then forms an M-ary symbol stream. That is, each M-ary symbol conveys m bits of processed data, where

$$M = 2^m \tag{2.1}$$

The size of the symbol alphabet is M and the symbol rate is 1/mth the processed data rate.

The MFSK modulator shifts a basic carrier at frequency f_c to one of M frequencies, each corresponding to one of the M possible symbols. Each such RF tone constitutes a "chip" of duration T_c, which is related to the chip rate R_c by

$$T_c = 1/R_c \tag{2.2}$$

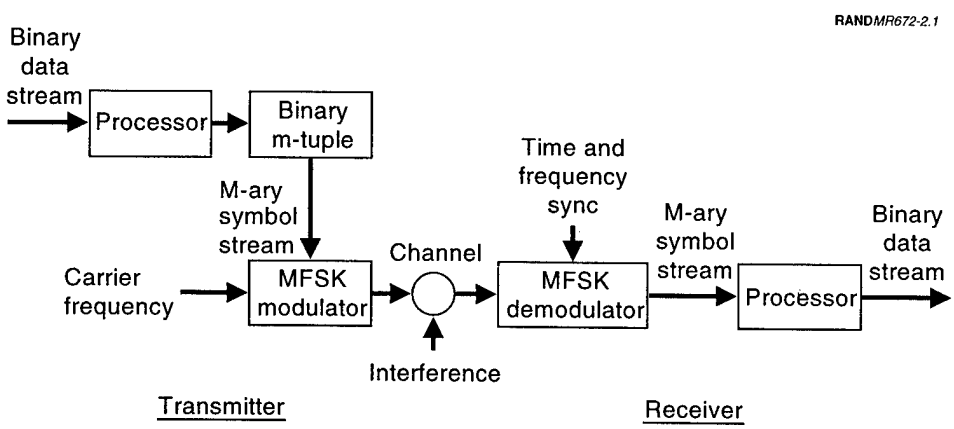

Figure 2.1—Basic MFSK System Block Diagram

The M carrier frequencies used to define the symbol alphabet can be resolved unambiguously by the MFSK receiver if they are separated by an integer multiple of R_c in frequency. This is illustrated in Figure 2.2 for M = 8 using minimum chip spacing.[1]

To form the frequency-hopped, spread-spectrum version of MFSK, the system block diagram takes the form shown in Figure 2.3. The difference is the addition of an FH modulator in the transmitter and an FH demodulator in the receiver, each controlled by a binary K-tuple buffer driven by identical pseudo-random sequences. During each chip interval, K of the binary digits generated by the pseudo-random-sequences generator are stored in the binary K-tuple buffer and used in the multiplier to select, apparently at random, one of 2^K carrier frequencies to which the basic MFSK carrier frequency f_c is hopped. The 2^K carrier frequencies are spaced M/R_c apart, with the result that the basic MFSK set of tones, which originally spanned a band of width M/R_c, will, over time, be observed to hop over a band of width $2^K M/R_c$. In the receiver, an identical pseudo-random sequence having a time delay equal to the propagation time "dehops" the various chips back to the basic MFSK carrier frequency, thereby permitting conventional MFSK demodulation.

The frequency-hopped, spread-spectrum version of the MFSK chip sequence presented in Figure 2.2 is depicted in Figure 2.4. The dashed line shown in each chip interval represents the hopped center frequency, which is displaced from the center frequency according to the pattern displayed in Figure 2.2. In terms of frequency slots that the chips can occupy, it is seen that there are a total of $2^K M$ over the spread band.

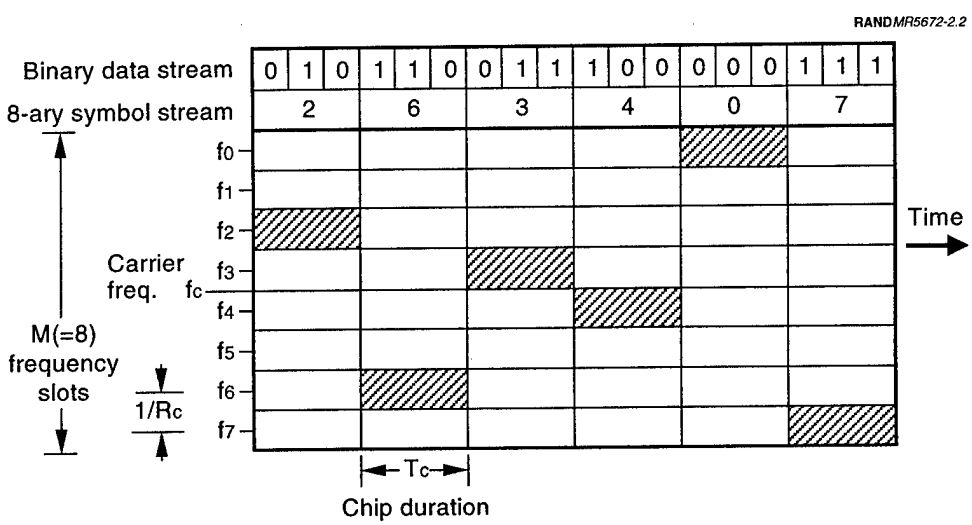

Figure 2.2—Frequency-Time Diagram of a Typical MFSK Chip Sequence for M = 8 with Minimum Chip Spacing in Frequency

[1]The shaded areas for the chips in Figure 2.2 suggest a time-bandwidth product of unity. The energy for each chip is indeed confined to its duration in time, but the distribution in frequency varies as $(\sin x/x)^2$ rather than being confined to $1/R_c$, as drawn.

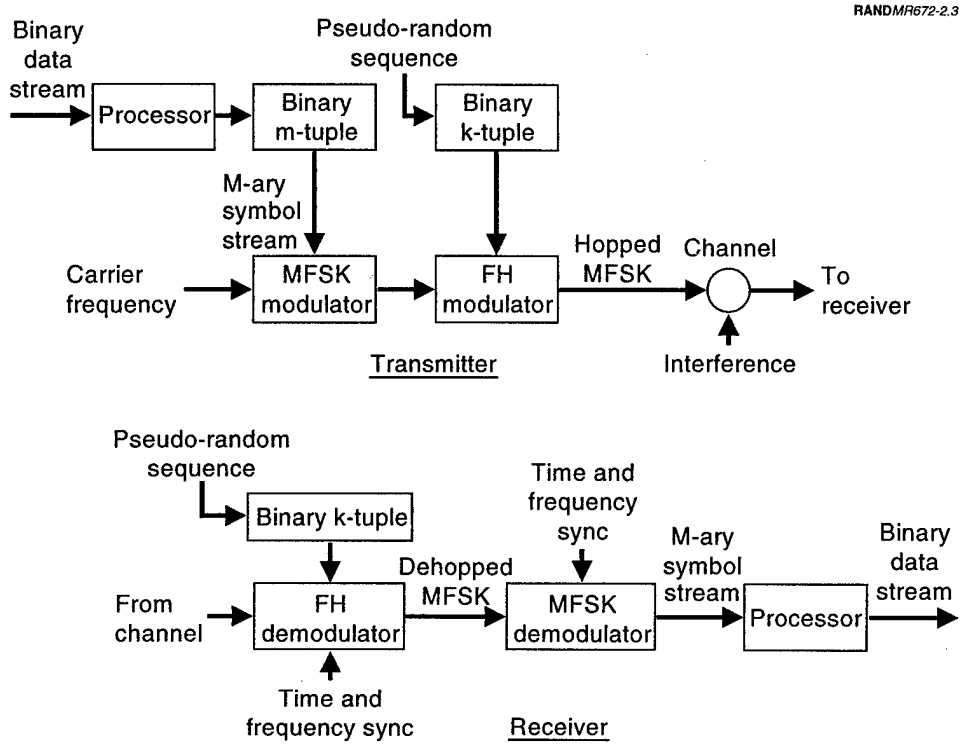

Figure 2.3—Basic FH MFSK System Block Diagram

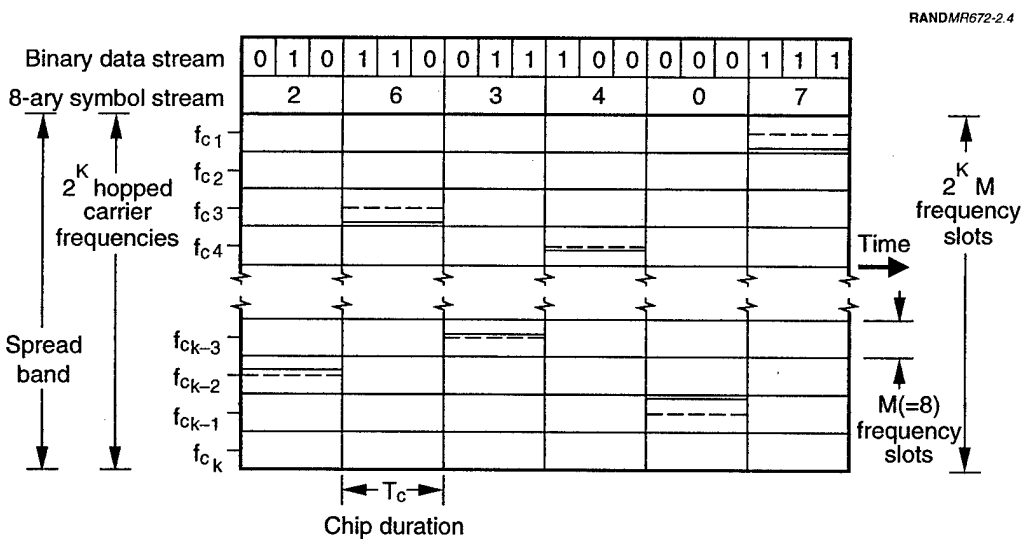

Figure 2.4—Frequency-Time Diagram of the FH MFSK Chip Sequence Shown in Figure 2.2 for M = 8

A final point has to do with the relationship between the symbol, chip, and hop rates. To simplify the demodulator design, both m, the number of bits per symbol (and, hence, the symbol alphabet size M), and the chip rate R_c are often fixed. When the symbol rate equals the chip rate the result is as shown in Figure 2.2, in which information is transmitted, at the rate of one symbol per chip. It is further customary to fix the hop rate equal to the chip rate with the result, as shown in Figure 2.4, of the transmission of one symbol per hopped chip.

In such systems the information rate in symbols per second is varied by changing the number of symbols per chip. Thus, the information rate can be doubled by sending two symbols per chip or halved by using two chips to send one symbol. Clearly, there must be a commensurable (preferably an integer) relationship between the symbol and chip rates; in practice, they are usually related by powers of 2.

For example, consider a system having a chip rate of 1600 per sec using M = 8 and rate 1/2 coding. In that case, an information rate of 2400 bps will result in a symbol rate of 1600 per sec, which matches the chip rate. Data rates of 1200, 600, 300, 150, and 75 bps will yield symbol rates of 800, 400, 200, 100, and 50 per sec and result in the transmission of 2, 4, 8, 16, and 32 chips for each symbol, respectively. When frequency-hopped, as shown in Figure 2.5, such systems are known as fast-frequency-hopped (FFH) because there may have to be a number of hops (up to 32 in this example), each consisting of one chip, to convey a given symbol. That is, the hop rate must equal or exceed the chip rate. The number of chips per symbol is also known as the order of diversity N. The dual diversity case, i.e., N = 2, illustrated in Figure 2.5 shows how pairs of hopped chips have identical displacements from the nominal hopped carrier frequencies.

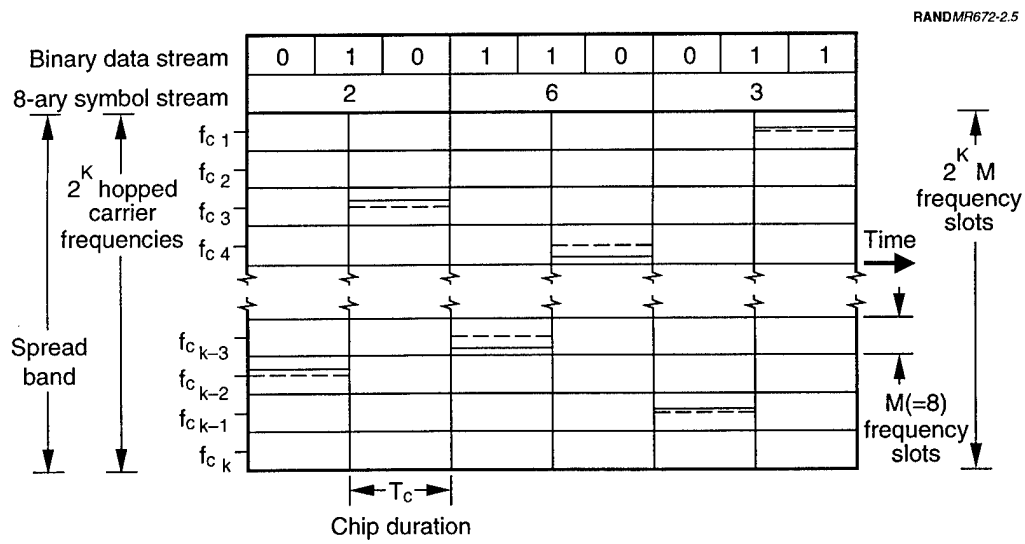

Figure 2.5—Frequency-Time Diagram of the FFH MFSK Chip Sequence Shown in Figure 2.2 for M = 8 and N = 2

The counterpart approach of slow-frequency-hopped (SFH) will not be described in detail here because the focus of the analysis to follow is on fast-frequency-hopping. More complete descriptions of both types can be found in Ziemer and Peterson (1985), Sklar (1988), and Simon et al. (1985).

THE HOPPED-SIGNAL ENVIRONMENT IN THE SPREAD BAND

Let n denote the number of frequency slots available in the spread band, where

$$n = 2^K M \tag{3.1}$$

as depicted in Figures 2.4 and 2.5, and assume that there are k users hopping about these n frequency slots. The hopped tones are assumed to be in time synchronization and approximate frequency-synchronization so that all users change hop frequencies at the same time and are approximately at the center frequencies of their associated frequency slots (but with random phases). Finally, it is assumed that the hops of the k users are uniformly distributed at random over the n frequency slots. Thus, the probability p that a given user will hop onto (or "hit") a given frequency slot is given by

$$p = \frac{1}{n} \tag{3.2}$$

Consider a given chip interval during which a total of k users are distributed at random among the n frequency slots. The probability $p(r_1, r_2, \cdots, r_n)$ that there will be r_i users in the ith frequency slot $i = 1, 2, \cdots, n$ is given by the multinomial distribution

$$p(r_1, r_2, \cdots, r_n) = \frac{k!}{r_1! r_2! \cdots r_n!} p_1^{r_1} p_2^{r_2} \cdots p_n^{r_n} \tag{3.3}$$

where p_i is the probability of a given user hopping into the ith frequency slot and

$$\sum_{i=1}^{n} p_i = 1 \qquad \sum_{i=1}^{n} r_i = k \tag{3.4}$$

When $p_i = 1/n$ for all i as in Eq. (3.2), Eq. (3.3) reduces to

$$p(r_1, r_2, \cdots, r_n) = \frac{k!}{r_1! r_2! \cdots r_n!} p^k \tag{3.5}$$

here because the demodulator at a given user needs only consider M of the frequency slots at a time, where, typically, $M << n$. It will be assumed, in that event, that the occurrences of users hopping into the M frequency slots are independent events so that Eq. (3.5) can be written.

$$p(r_1, r_2, \cdots, r_n) = p(r_1)p(r_2)\cdots p(r_n) \tag{3.6}$$

The individual probabilities that r of the k users are to be found in a given frequency slot are then given by the binomial distribution

$$p(r) = \frac{k!}{r!\,(k-r)!} p^r (1-p)^{k-r} \qquad r=1, 2, \cdots, k \tag{3.7}$$

where p is the probability of a user hopping into the frequency slot of interest and $1 - p$ is the probability of the user hopping elsewhere. The average λ of r in Eq. (3.7) is given by

$$\lambda = kp = k/n \tag{3.8}$$

where Eq. (3.2) has been used.

A further simplification is possible by noting that in the limit as $k \to \infty$ (many users) and $p = 1/n \to 0$ (many frequency slots) in such a way that λ, the average number of users hopping into a given frequency slot, as given by Eq. (3.8), remains constant, it can be shown (e.g., Cramér, 1946) that Eq. (3.7) approaches a Poisson distribution

$$p(r) = \frac{\lambda^r e^{-\lambda}}{r!} \qquad r = 0, 1, 2, \cdots \tag{3.9}$$

It will be assumed that this approximation is valid for this analysis.

From the communication point of view, it is preferable to consider one of the k users as the desired one and the other $k - 1$ users as potential interferers. Hence, when one considers the M frequency slots of interest to an MFSK receiver, it can be assumed that each of them will contain r interfering tones, where r has the distribution given by Eq. (3.9), but with

$$\lambda = \frac{k-1}{n} \tag{3.10}$$

and that one of them will contain the desired tone as well. An alternative formulation for λ is obtained by noting that the total number of frequency slots n is equal to the hopping bandwidth W divided by the bandwidth R_c per frequency slot. Hence,

$$\lambda = \frac{(k-1)R_c}{W} = \frac{k-1}{WT_c} \tag{3.11}$$

where Eq. (2.2) has been used to introduce the chip duration T_c in preference to R_c.

Chapter Four

THE MFSK DEMODULATOR

There are a variety of MFSK demodulators used in pratical MFSK receivers. The block diagram of the MFSK demodulator chosen for analysis is shown in Figure 4.1. Though optimum for use in the presence of wideband noise, it was not chosen for this reason. The interference to be considered here includes the possibility of multiple interfering tones from other users, as well as tone jamming, a condition for which the optimum demodulator structure is not known. Future analysis may require consideration of other structures.

It is assumed that the hopped signal shown in Figures 2.4 or 2.5 has been dehopped and converted to a convenient intermediate frequency (IF). The detection is done in a bank of M non–coherent, quadrature detectors, each tuned to one of the M symbol frequencies. An operator f at the output of each detector defines its basic characteristic. For an amplitude detector, sometimes called a linear detector, $f(\Sigma)=\sqrt{\Sigma}$; for a square-law detector $f(\Sigma)=\Sigma$. In principle, any monotone function f can be used. The M detection channels each contain such a detector whose output $f(\Sigma)$ is sampled at the end of each chip interval, T_c. These samples are then summed over the N chip intervals constituting a symbol and presented to the symbol detector, which selects the largest sum as the best estimate of the transmitted symbol.

In a simple communication link, the input would consist, at any given time, of a desired tone to which is added background noise. Thus, one of the M detectors will experience that tone plus noise as its input and the remaining M – 1 will have noise alone. The analysis of such a system is well known and can be found in any standard text. The interest here is in a system in which, in addition to the background noise, M – 1 of the detectors experience a number of extraneous tones and one detector experiences noise, the extraneous tones, and the tone from the desired user. The calculation of the symbol error probability in such a case is much more difficult and no general solution is available. The analysis offered here treats the tractable special case in which the extraneous tones can be treated as two-dimensional gaussian variates.

It should be noted that the quadrature detectors shown in Figure 4.1 are not slab-sided, bandpass filters having a bandwidth equal to that of the frequency slot to which they are tuned. In fact, their frequency responses are of the sin x/x form, which means that they will respond significantly to tones well outside the frequency slot to which they are tuned. This property is accommodated in practice by making

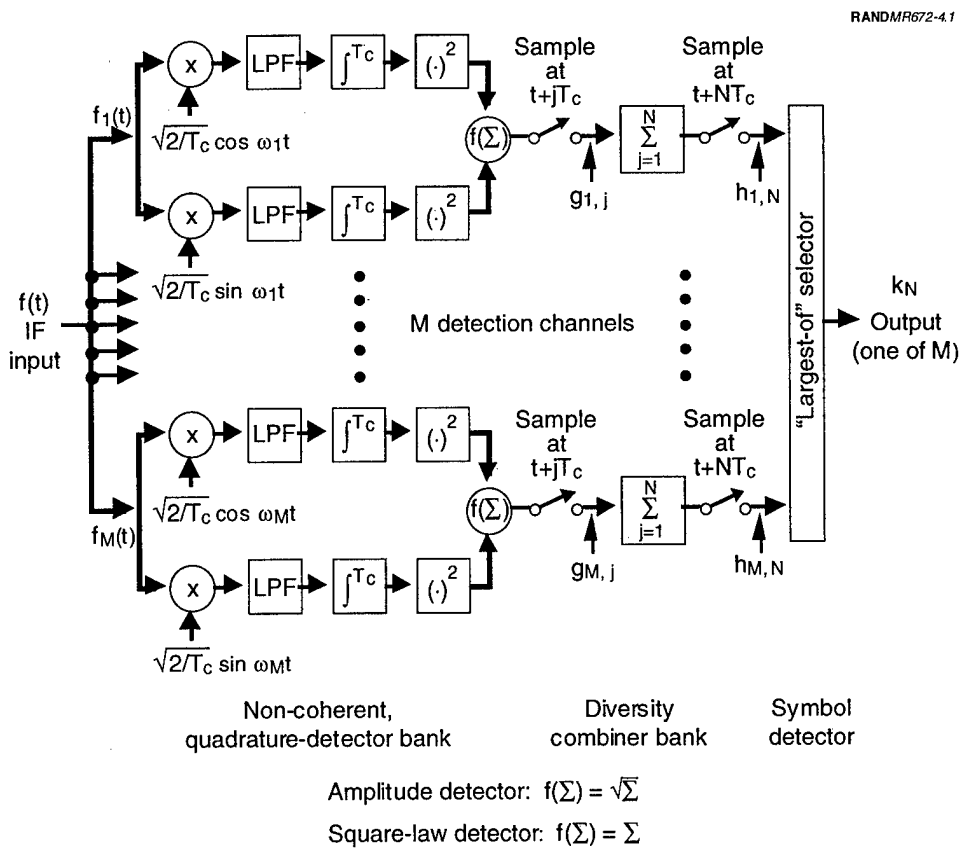

Figure 4.1—Typical Fast-Frequency-Hopping MFSK Demodulator

the integration time equal to the chip length, with the result that, if the quadrature detectors are all tuned to the centers of the frequency slots they are intended to cover, then the zeros of their individual sin x/x frequency responses will all fall at the centers of the other frequency slots. Hence, the only quadrature detector that will respond to a tone centered on a given frequency slot is the one tuned to that frequency slot. The quadrature detectors are then said to be orthogonal. Actually, orthogonality is realized for any set of M frequency slots to which the quadrature detectors are tuned, not just the adjacent sets illustrated in Figures 2.2, 2.4, and 2.5. Non-adjacent sets are sometimes used to diminish the effect of non-centered tones in nearby frequency slots by taking advantage of the sin x/x frequency-response falloff. The term "modulation index" is sometimes used to describe this practice, with a modulation index of unity denoting the use of adjacent frequency slots, a modulation index of two denoting the use of every other frequency slot, etc.[1]

[1]The term "modulation index" is also widely used to express the ratio of frequency deviation of a frequency modulated carrier to the frequency of a sinusoidal modulating signal.

present, the same would be true of a randomly hopped, FH MFSK system, the only difference being that coordinated dehopping is required to present the contents of the M frequency slots then of interest to the quadrature detector bank during each chip interval. If the interfering tones in the M frequency slots were also at the centers of their frequency slots, they would, like the desired tone, be accepted only by their corresponding quadrature detectors. It will be assumed in the following that despite oscillator instabilities, Doppler shifts, etc., all of the tones are sufficiently close to the center frequencies of their associated frequency slots that mutual effects on other quadrature detectors can be neglected.[2] In other words, each quadrature detector will be assumed to have at its input only those tones present in the frequency slot to which it is tuned. Furthermore, it will be assumed that the receiver has attained frequency synchronization with the desired tone. That is, the quadrature oscillator in each quadrature detector is at exactly the same frequency that the desired tone would have were it input to that quadrature detector.

Hence, as indicated on Figure 4.1, the total input to the MFSK demodulator can be written as

$$f(t) = \sum_{i=1}^{2^K M} f_i(t) \tag{4.1}$$

where $f_i(t)$ represents only the sum of the tones present in the ith frequency slot. Only M of these $2^K M$ frequency slots are of interest to the MFSK demodulator. The input to the kth of these M detection channels can then be written

$$f_k(t) = \sum_{i=1}^{\rho_k} a_i \cos(\omega_i t + \theta_i) \qquad k = 1, 2, \cdots, M \tag{4.2}$$

where the summation indicates that there are ρ_k terms present. If the kth detection channel is the one containing the desired tone, ρ_k will equal $r + 1$, where r is a Poisson random variable drawn from Eq. (3.9) with a mean given by Eq. (3.10). If the kth detection channel does not contain the desired tone, ρ_k will simply equal r.

Even if the users have approximately equal radiated powers (as a result, perhaps, of system power control), the received tones will have amplitudes a, which, though relatively constant as a function of time, may differ considerably from one another for practical reasons, and may resemble random variables. The radian frequencies, i.e., the ω, will correspond approximately to the M permissible tone frequencies to which the detectors are tuned. As noted above, the frequency of the desired tone will match exactly, but the $k - 1$ others will differ slightly from the corresponding quadrature-detector frequencies because of oscillator instabilities and Doppler shifts. Lacking phase synchronization, the θ will be random variables uniformly

[2]This is a practical assumption in an FH system using a satellite as a communications relay. It could be implemented by using a beacon aboard the satellite as a reference, for example.

distributed in $(0,2\pi)$. It will be assumed in the following that a, ω, and θ remain essentially constant during a chip interval.

Consider the kth detection channel $(k = 1,2,\cdots,M)$ at the end of the jth diversity chip $(j = 1,2,\cdots,N)$. It is shown in Appendix A that the output of the first sampler in Figure 4.1 is given by

$$g_{k,j} = f\left\{\sum_{i=1}^{\rho_k} \frac{a_i^2 T_c}{2}\left(\frac{\sin x_i}{x_i}\right)^2 + 2\sum_{\substack{i=1\\ i\neq j}}^{\rho_k}\sum_{j=1}^{\rho_k} \sqrt{\frac{a_i^2 T_c}{2}}\left(\frac{\sin x_i}{x_i}\right)\sqrt{\frac{a_j^2 T_c}{2}}\left(\frac{\sin x_j}{x_j}\right)\cos\left[(x_i - x_j) + (\theta_i - \theta_j)\right]\right\} \tag{4.3}$$

where

$$x_i = (\omega_i - \omega_k)\,T_c/2 \qquad x_j = (\omega_j - \omega_k)\,T_c/2 \tag{4.4}$$

and f is defined in Figure 4.1 for the particular type of detector being considered.

If, for a square-law quadrature detector, for which $f(\Sigma) = \Sigma$, only a single properly tuned tone of amplitude a is present, Eq. (4.3) reduces to

$$g_{k,j} = \frac{a^2 T_c}{2} \tag{4.5}$$

If the tone has power P, its amplitude is given by

$$a = \sqrt{2P} \tag{4.6}$$

and its energy by

$$E_c = PT_c = \frac{a^2 T_c}{2} \tag{4.7}$$

which shows, from comparison with Eq. (4.5), that the square-law, quadrature detector is a true energy detector when only a single tone is present. However, if there are two or more tones arriving with different amplitudes, frequencies, and phases, the cross terms and sin x/x factors in Eq. (4.3) arise and the output of a square-law, quadrature detector is seen to be other than the sum of the energies of the component tones. Quadrature detectors of other types, e.g., linear, are not energy detectors even when the input is a single properly tuned tone.

Fortunately, the form of $g_{k,j}$ can be made more tractable in the multi-tone case by taking advantage of the assumption of approximate frequency-synchronization of

the extraneous tones in each quadrature detector. In that case, the composite signal that is input to each of the quadrature detectors, being the sum of r (or r + 1) tones of independent random phase and amplitude at approximately the same frequency, will not appear to change significantly in total amplitude or phase during the integration time T_c. Then, each quadrature detector output will be given approximately by

$$g_{k,j} = f\left(\frac{a^2 T_c}{2}\right) \tag{4.8}$$

as if there were only a single tone of composite amplitude a at its input.

Determining the amplitude distribution of this composite tone requires finding the magnitude of the sum of its two-dimensional component tones. In general, this is a difficult computation, particularly when more than only a few tones are involved. It will be seen in Chapter Six, however, that an especially simple solution results when the component tones are assumed to be two-dimensional Gaussian variates. In that event, the individual tones, as well as their sums, have Rayleigh amplitude distributions.

Finally, the output of the second sampler in the kth detection channel in Figure 4.1 is given by

$$h_{k,N} = \sum_{j=1}^{N} g_{k,j} \qquad k = 1,2,\cdots,M \tag{4.9}$$

Let k_N identify the detection channel that has the largest value of $h_{k,N}$, i.e.,

$$k_N \equiv \max h_{k,N} \tag{4.10}$$

This, then, identifies the detection channel most likely to contain the transmitted symbol.

Chapter Five

THE SYMBOL ERROR PROBABILITY

In a conventional communications application, analysis of the performance of an MFSK demodulator is considerably simplified because the interference consists solely of a relatively weak Gaussian background noise that appears equally in all the M detection channels. In the application of interest here, in which the interference consists of random noise plus a number of extraneous tones from other users, the presence and distribution of these extraneous tones must be considered carefully, because they can be expected to be comparable in amplitude to the desired tone.

With reference to Figure 4.1, consider the set of MN interfering tones that will be incident upon the MFSK demodulator in the course of the N chips that constitute the single symbol to be transmitted by Nth-order diversity. Let $r_{k,j}$ denote the number of interfering tones present in the kth detection channel during the jth chip, where $k = 1,2,\cdots,M$ and $j = 1,2,\cdots,N$, and where $r_{k,j}$ is a random variable chosen from the Poisson distribution given by Eq. (3.9). It may be assumed, without loss of generality, that the desired tone is contained in the Mth detection channel. Thus, in the first $M - 1$ detection channel, there will be only interfering tones, whereas in the Mth detection channel, there will be interfering tones plus the desired tone. To determine the probability of correctly identifying the Mth channel as the one containing the desired tone, it is necessary to consider the probability density functions of these ensembles of tones.

Consider first the $M - 1$ detection channels not containing the desired tone. Let $\pi(g_{k,j})$ denote the probability density function of the output of the first sampler in the kth detection channel at the end of the jth diversity chip where $g_{k,j}$ is given by Eq. (4.8) for $k = 1,2,\cdots,M-1$. Clearly, $\pi(g_{k,j})$ has the same functional form in all $M - 1$ detection channels for each of the N diversity chips, the only difference in a particular chip being the parameter of the distribution as determined by the number of interfering tones that are present. Then, let $p(h_{k,N})$ denote the probability density function of the output of the second sampler in the kth detection channel at the end of the Nth diversity chip, where $h_{k,N}$ is given by Eq. (4.9). It is apparent from Eq. (4.9) that $p(h_{k,N})$, $k = 1,2,\cdots,M-1$ is simply the N-fold convolution of the $\pi(g_{k,j})$.

Consider next the Mth detection channel, which contains in each chip both the desired tone and interfering tones. Let $\phi(g_{M,j})$ denote the probability density function of the output of the first sampler at the end of the jth diversity chip, where $g_{k,j}$ is given by Eq. (4.8) for $k = M$. Clearly, $\phi(g_{M,j})$ has the same functional form in each of the N diversity chips, the only difference in a particular chip being the parameter of

the distribution as determined by the number of interfering tones that are present. Then, let $f(h_{M,N})$ denote the probability density function of the output of the second sampler at the end of the Nth diversity, where $h_{M,N}$ is given by Eq. (4.9) for $k = M$. As was the case for the $M - 1$ non-signal-bearing channels, $f(h_{M,N})$ is the N-fold convolution of the $\phi(g_{M,j})$.

The probability $\wp_e^s(M,N)$ of symbol error in a MFSK system using Nth-order diversity for a particular set $[r_{k,j}]$ of interfering tones is found by calculating the probability that an incorrect decision is made as to which detection channel contains the desired tone. This decision is made on the basis of which detection channel has the largest output at the end of the diversity transmission. Given that the desired tone is in the Mth detection channel, a correct decision will be made if $h_{M,N}$, the output of Mth detection channel, is the greatest of the outputs $h_{k,N}$, $k = 1,2,\cdots,M-1$ of the other $M - 1$ detection channels. For convenience, let x_k denote $h_{k,N}$. Then, the probability of a correct decision is given by

$$P_c(x_M) = P(\text{all } x_k < x_M) \quad k = 1,2,\cdots,M-1 = \prod_{k=1}^{M-1} \int_0^{x_M} p(x_k)dx_k \tag{5.1}$$

The probability of symbol error $\wp_e^s(M,N)$ for this particular set $[r_{k,j}]$ of interfering tones is found by averaging $[1-P_c(x_M)]$ over the probability density function $f(x_M)$. Hence,

$$\begin{aligned}\wp_e^s(M,N) &= \int_0^\infty f(x_M)\left[1-\prod_{k=1}^{M-1}\int_0^{x_M} p(x_k)dx_k\right]dx_M \\ &= 1-\int_0^\infty f(x_M)\prod_{k=1}^{M-1}\left[1-\int_{x_M}^\infty p(x_k)dx_k\right]dx_M\end{aligned} \tag{5.2}$$

Expanding the product yields

$$\begin{aligned}\wp_e^s(M,N) = 1-\int_0^\infty f(x_M)\Bigg[&1-\sum_{k_1=1}^{M-1}\int_{x^M}^\infty p(x_{k_1})dx_{k_1} \\ &+\sum_{k_1=1}^{M-1}\sum_{\substack{k_2=1\\k_1\neq k_2}}^{M-1}\int_{x_M}^\infty p(x_{k_1})dx_{k_1}\int_{x_M}^\infty p(x_{k_2})dx_{k_2}-\cdots \\ &+(-1)^{M-1}\sum_{k_1=1}^{M-1}\sum_{\substack{k_2=1\\k_1\neq k_2\neq\cdots\neq k_{M-1}}}^{M-1}\cdots\sum_{k_{M-1}=1}^{M-1}\int_{x_M}^\infty p(x_{k_1})dx_{k_1}\int_{x_M}^\infty p(x_{k_2})dx_{k_2}\cdots \\ &\int_{x_M}^\infty p(x_{k_{M-1}})dx_{k_{M-1}}\Bigg]d_{x_M}\end{aligned}$$

which leads to

$$\begin{aligned}\wp_e^s(M,N) = &\sum_{k_1=1}^{M-1}\int_0^\infty f(x_M)\left[\int_{x_M}^\infty p(x_{k_1})dx_{k_1}\right]dx_M \\ &-\sum_{\substack{k_1=1\\k_1\neq k_2}}^{M-1}\sum_{k_2=1}^{M-1}\int_0^\infty f(x_M)\left[\int_{x_M}^\infty p(x_{k_1})\,dx_{k_1}\int_{x_M}^\infty p(x_{k_2})\,dx_{k_2}\right]dx_M + \cdots \\ &(-1)^{M-1}\sum_{k_1=1}^{M-1}\sum_{\substack{k_2=1\\k_1\neq k_2\neq\cdots\neq k_{M-1}}}^{M-1}\cdots\sum_{k_{M-1}=1}^{M-1}\int_0^\infty f(x_M) \\ &\left[\int_{x_M}^\infty p(x_{k_1})dx_{k_1}\int_{x_M}^\infty p(x_{k_2})dx_{k_2}\cdots\int_{x_M}^\infty p(x_{k_{M-1}})dx_{k_{M-1}}\right]dx_M\end{aligned} \tag{5.3}$$

For binary FSK (i.e., M = 2), only the leading term exists. Hence, the probability of symbol error becomes

$$\wp_e^s(2,N) = \int_0^\infty f(x_2)\left[\int_{x_2}^\infty p(x_1)dx_1\right]dx_2 \tag{5.4}$$

When it is inconvenient to use the complete expansion given by Eq. (5.3) or the integrals in Eq. (5.2) are intractable, a union bound (Stiffler, 1971) can often be used. This is done by noting that for $M \geq 3$ the probability of error $\wp_e(M,N)$ given by Eq. (5.2) considers the probability that the output of *any* of the non-signal-bearing channels will exceed that of the signal-bearing channel. Hence, it is bounded below by the probability that the exceedance will occur *only* in the non-signal-bearing channel in which an exceedance is most likely to occur. Similarly, it is bounded above by the probability that exceedances will occur in *all* of the non-signal-bearing channels. A weaker upper bound is given by M – 1 times the probability of an exceedance in the non-signal-bearing channel in which an exceedance is most likely to occur.

To formulate these bounds, let $\Pr(x_k \geq x_M)$ $k = 1, 2, \cdots, M-1$ denote the probability of an exceedance in the kth (non-signal-bearing) detection channel. Then,

$$\max_k \Pr(x_k \geq x_M) \leq \wp_e^s(M,N) \leq \sum_{k=1}^{M-1} \Pr(x_k \geq x_M)$$
$$\leq (M-1) \max_k \Pr(x_k \geq x_M) \tag{5.5}$$

(It should be noted that the right-most term can exceed unity so it is not a true probability.) Applying Eq. (5.5) to Eq. (5.2) and considering only the left-hand upper bound yields.

$$\wp_e^s(M,N) \leq \sum_{k=1}^{M-1} \left\{ 1 - \int_0^\infty f(x_M) \left[1 - \int_{x_M}^\infty p(x_k)dx_k \right] dx_M \right\} = \sum_{k=1}^{M-1} \int_0^\infty f(x_M) \left[\int_{x_M}^\infty p(x_k)dx_k \right] dx_M \tag{5.6}$$

which is seen to be the leading term in Eq. (5.3). If, as is the case in conventional MFSK systems, the non-signal-bearing detection channels contain only equal amounts of noise, the upper bounds in Eq. (5.5) become equal and it is possible to write

$$\wp_e^s(M,N) \leq (M-1) \int_0^\infty f(x_M) \left[\int_{x_M}^\infty p(x_k)dx_k \right] dx_M \tag{5.7}$$

which is valid for $\wp_e^s(M,N) << 1$.

In the FH MFSK system being considered here, the non-signal-bearing detection channels may contain either no interference at all or interference in the form of one or more tones. At low orders of diversity, when only a few interfering tones are present, the probability of an exceedance can differ greatly from one non-signal-bearing detection channel to another. Hence, the right-hand upper bound in Eq. (5.5) can easily become meaningless.

The left-hand upper bound might suffice, but it, too, might become meaningless. This comes about because the presence of even one interfering tone in a non-signal-bearing channel will lead to an error probability on the order of 1/2 if it is comparable in amplitude to the desired tone. Hence, the presence of one tone in each of only two of the non-signal-bearing channels can lead to an upper probability bound exceeding unity.

Finally, it should be recalled that $\wp_e(M,N)$ is the probability of error for a particular set $[r_{k,j}]$ of interfering tones. The overall probability of symbol error $\wp_e(M,N)$ is then found by averaging $\wp_e(M,N)$ over all possible sets of interfering tones that can occur. Thus,

$$P_e^s(M,N) = \sum_{r_{1,1}=0}^{\infty} \sum_{r_{1,2}=0}^{\infty} \cdots \sum_{r_{M,N}=0}^{\infty} p(r_{1,1})p(r_{1,2})\cdots p(r_{M,N})\wp_e^s(M,N) \tag{5.8}$$

where, from Eq. (3.9), it is seen that

$$p(r_{1,1})p(r_{1,2})\cdots p(r_{M,N}) = \frac{\lambda^{(r_{1,1}+r_{1,2}+\cdots+r_{M,N})} e^{-\lambda MN}}{r_{1,1}!\, r_{1,2}!\cdots r_{M,N}!} \tag{5.9}$$

in which λ is given by Eq. (3.10) or Eq. (3.11). It is customary to present final results in terms of bit, rather than symbol, error probability. Viterbi (1966) shows that

$$P_e^b = \frac{M}{2(M-1)} P_e^s \tag{5.10}$$

which may be used to convert Eq. (5.8).

AN ANALYTICAL MODEL FOR USER INTERFERENCE

The essence of the theory leading to Eq. (5.2) for the symbol error probability is that the interfering tones from other system users can be regarded as having independent random amplitudes. Accordingly, an analytical solution can be found only if: first, the probability density function of the amplitude of the sum of such tones is a relatively simple function of the probability density functions of the individual tones (this leads to the probability density function of the $g_{k,j}$ in Eq. (4.8)); second, that the probability density function of the sum of the sums is relatively simple (this leads to the probability density function of the $h_{k,N}$ in Eq. (4.9)); and third, that this latter probability density function, termed p(x) in Eq. (5.3), leads to tractable integrals. However, to be of practical value, the probability density function of the amplitudes of the individual interfering tones must also be reasonably realistic. Unfortunately, one can only speculate on what constitutes realism because few, if any, quantitative measurements exist.

One probability density function, which is particularly suitable for the non-diversity case (in which there is only one term in Eq. (4.9)), has been identified. It stems from the assumption that the individual interfering tones can be approximated as two-dimensional Gaussian variates. That is, that they can be written

$$f(t) = X\cos\omega t + Y\sin\omega t \tag{6.1}$$

where X and Y are Gaussian with mean, zero, and variance σ^2 and where ω denotes an arbitrary carrier frequency. In this case, the variance σ^2 also equals the power P of f(t).

A more convenient form for f(t) is given by

$$f(t) = A\cos(\omega t + \theta) \tag{6.2}$$

where A is a Rayleigh variable with a probability density function

$$P_A(A) = \frac{A}{P}\exp\left(-\frac{A^2}{2P}\right) \qquad A \geq 0 \tag{6.3}$$

and θ is an independent random variable uniformly distributed in $(0,2\pi)$. The second moment of A is

$$\overline{A^2} = 2P \tag{6.4}$$

which accords with the fact that

$$\overline{f^2(t)} \equiv P = \frac{1}{2}\overline{A^2} \tag{6.5}$$

A normalized form of Eq. (6.3) obtained by setting

$$\alpha = A/\sqrt{P} \tag{6.6}$$

to obtain

$$P_\alpha(\alpha) = \alpha \exp(-\alpha^2/2) \tag{6.7}$$

which is plotted in Figure 6.1 for convenience.

Inasmuch as the individual interfering tones are Gaussian $(0, \sigma^2)$ in accordance with Eq. (6.1), the sum of r such tones is Gaussian $(0, r\sigma^2)$. As a result, the probability density function of the amplitude a of the sum of r tones becomes, from Eq. (6.3),

$$p_a(a) = \begin{cases} \delta(a) & r = 0 \\ \dfrac{a}{rP}\exp\left(-\dfrac{a^2}{2rP}\right) & r = 1, 2, \cdots \end{cases} \qquad a \geq 0 \tag{6.8}$$

where $\delta(x)$ is the Dirac delta function.

When, in addition to the r interfering tones, which are Gaussian and whose sum has an amplitude having the probability density function given by Eq. (6.8), there is also additive Gaussian noise of power spectral density N_0, the total amplitude is again Gaussian but with a probability density function given by

$$p_a(a) = \frac{a}{(rP + N_0/T_c)} \exp\left[\frac{-a^2}{2(rP + N_0/T_c)}\right] \qquad r = 0, 1, 2, \cdots \qquad a \geq 0 \tag{6.9}$$

where N_0/T_c is the average noise power during a chip of duration T_c.

To show that Eq. (6.3) is a reasonable approximation to the probability density function of the individual amplitudes of the ensemble of system users in a realistic situation, consider the experimental data published by Viterbi (1994) and shown in Figure 6.2. The received E_b/I_0, where E_b is the energy per bit and I_0 is the total interference, for a terrestrial CDMA cellular system employing power control is seen to closely resemble a normal distribution. (Inasmuch as the total interference in such a system is virtually constant, E_b/I_0 is effectively a measure of signal power.) Viterbi notes that the distribution has a standard deviation of less than 2.5 dB.

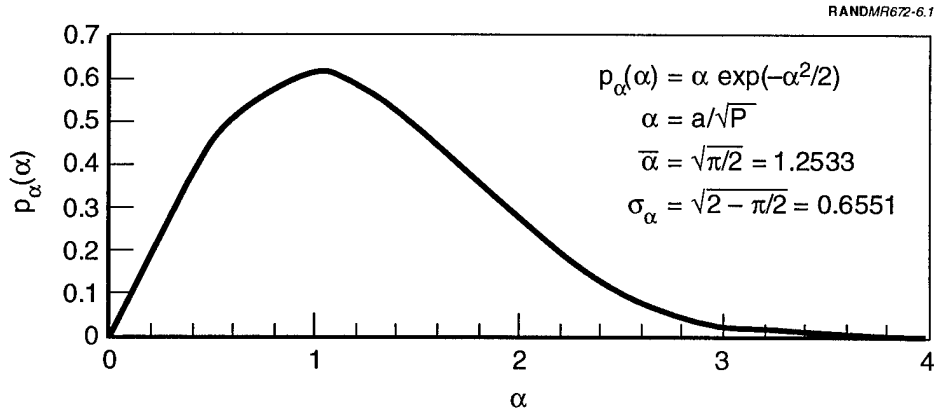

Figure 6.1—Probability Density Function of Normalized Rayleigh Variable

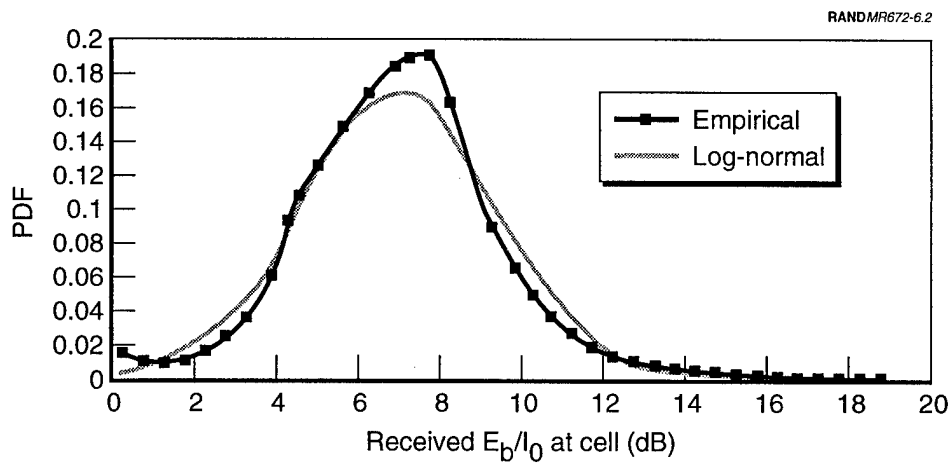

SOURCE: Andrew J. Viterbi, "The Orthogonal-Random Waveform Dichotomy for Digital Mobile Personal Communication," *IEEE Personal Communications*, Vol. I, No. 1, First Quarter, 1994, pp. 18–24. © 1994 IEEE.

Figure 6.2—Probability Density Function of E_b/I_0 dB for a Terrestrial CDMA Cellular System Employing Power Control

The corresponding comparison for the Rayleigh variable α as given by Eq. (6.7), can be made by considering its value in dB

$$\alpha_{dB} = 10\log_{10}\alpha \tag{6.10}$$

It is shown in Appendix B that the probability density function of α_{dB} is given by

$$p_{\alpha_{dB}}(\alpha_{dB}) = \frac{h}{20}\exp(h\alpha_{dB}/10)\exp\left[-\frac{1}{2}\exp(h\alpha_{dB}/10)\right] \quad -\infty < \alpha_{dB} < \infty \tag{6.11}$$

where

$$h = \log_e 10 = 2.30258\cdots \tag{6.12}$$

The mean and standard deviation of α_{dB} are equal to

$$\overline{\alpha_{dB}} = 0.50348 \quad \text{dB}$$

and

$$\sigma_{\alpha_{dB}} = 5.57004 \quad \text{dB} \tag{6.13}$$

This density function is plotted in Figure 6.3 together with a normal distribution having the same mean and variance.

A comparison of Figures 6.2 and 6.3 reveals a resemblance between Viterbi's measurements and the Rayleigh distribution. The principal difference between them appears to be that Viterbi's standard deviation is about 2.5 dB, whereas the standard deviation of the Rayleigh distribution is 5.57 dB. This difference of about 3 dB may be said to indicate that the power control in a system characterized by a Rayleigh distribution is less stringent than that in Viterbi's system. It would be desirable to be able to specify the standard deviation separately but this is not possible for the Rayleigh distribution because it has a fixed relationship between its mean and its standard deviation.

The comparison of Figures 6.2 and 6.3 also reveals a resemblance of both distributions to the log-normal distribution, which does have the property that the mean and the standard deviation can be specified separately. Unfortunately, Viterbi's measurements are the only ones at hand that pertain directly to the variability of

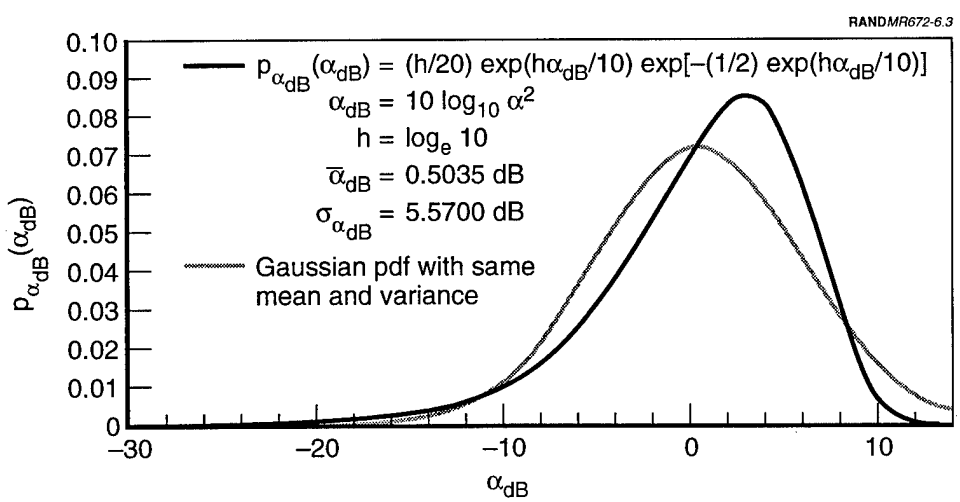

Figure 6.3—Probability Density Function of Normalized Rayleigh Variable in dB

received signal levels in a power-controlled system. Nonetheless, there are precedents for considering the log-normal distribution because it is used in specifying some aspects of signal losses in communication systems. For example, Fenton (1960) notes that the transmission loss in scatter propagation systems has been found to have a log-normal distribution. In another vein, Loo (1990) reports that the received signal from a satellite repeater when shadowed by foliage and modeled by a log-normal distribution shows a good comparison to measurements. A similar observation relating to the received signal in mobile radio systems is contained in French (1979).

Unfortunately, there is no obvious relationship between the variability displayed by a shadowed or scattered signal and that displayed by a signal resulting from imperfect power control. It would appear that more directly related measurements will be required before the use of a log-normal distribution can be justified. Consequently, the Rayleigh distribution will be used in the analysis to follow largely because of its similarity to Viterbi's measurements and the simplicity of analysis that it affords.

ANALYSIS OF THE NON-DIVERSITY CASE (N = 1)

The analytical model developed in the previous chapter is used here to analyze the non-diversity case. Thus, each chip will convey a given M-ary symbol by occurring at the appropriate one of the M signaling-alphabet tones. As mentioned in Chapter Five, the desired chip will be assumed to be in the Mth detection channel and all M channels will be equally subject to "hits" by interfering tones, where, in accordance with the development presented in Chapter Three, the probability of r interfering tones appearing in a given detection channel is given by Eq. (3.9).

The following analysis is done specifically for the linear, or amplitude, detector. However, it is clear that it is valid for any detector whose output is a monotone function of the quadrature-detector output. Hence, it applies to the square-law detector as well.

For the linear detector, the characteristic to be used is given in Figure 4.1 as $f(\Sigma)=\sqrt{\Sigma}$. Under the assumptions of time and frequency synchronization presented in Chapter Four, this causes the sum of the interfering tones and noise at the input to each detection channel to behave like a Rayleigh variable having a probability density function given by Eq. (6.9), where r is the number of interfering tones present. It is seen from Eq. (4.3) that the linear detector output is simply proportional to its input because only a single term equal to the square root of Eq. (4.5) remains. Hence, the probability density function of the linear-detector output $g_{k,j}$ can be found by making the change of variables given by the square root of Eq. (4.5) in Eq. (4.8). However, it is more convenient to consider a normalized output variable x_k given by

$$x_k = \frac{\sqrt{g_{k,j}}}{\sqrt{T_c P/2}} = \frac{a\sqrt{T_c/2}}{\sqrt{T_c P/2}} = \frac{a}{\sqrt{P}} \tag{7.1}$$

Then, the probability density function of the output of the kth non-signal-bearing, linear detector is found from Eq. (6.9) to be

$$p(x_k) = \sqrt{P}\, p_a(x_k\sqrt{P}) = \frac{x_k}{r_k + \frac{N_0}{PT_c}} \exp\left[-\frac{x_k^2}{2\left(r_k + \frac{N_0}{PT_c}\right)}\right] \qquad \begin{array}{l} r_k = 0, 1, 2, \cdots \\ k = 1, 2, \cdots, M-1 \end{array} \tag{7.2}$$

where the notation of Eq. (5.3) has been used. Note that the energy per chip E_c of the average interfering user is equal to PT_c, so the quantity N_0/PT_c is seen to be simply the reciprocal of the average chip signal-to-noise ratio E_c/N_0.

In the Mth, or signal-bearing, channel, the total input amplitude a will have the probability density function of sine wave plus noise given by Rice (1945) as

$$p_a(a) = \frac{a}{\sigma^2}\exp\left(-\frac{a^2+b^2}{2\sigma^2}\right)I_0\left(\frac{ab}{\sigma^2}\right) \qquad a,b \geq 0 \tag{7.3}$$

where b is the amplitude of the sine wave, σ^2 is the variance, or power, of the noise, and I_0 is a modified Bessel function of the first kind of order zero. In this case, the "noise" consists of the sum of the r_M interfering tones appearing in the Mth detection channel and the additive Gaussian noise of power N_0/T_c. Thus,

$$\sigma^2 = r_M P + N_0/T_c \tag{7.4}$$

where P is the average user power. Let the power of the tone from the desired user, which is equal to $b^2/2$, be a fraction f of the average power P. Then,

$$\frac{b^2}{2} = fP \tag{7.5}$$

Substituting Eqs. (7.4) and (7.5) into Eq. (7.3) and normalizing the amplitude a to the average power P according to Eq. (7.1) then leads to

$$f(x_M) = \frac{x_M}{r_M + \dfrac{N_0}{PT_c}}\exp\left[-\frac{x_M^2 + 2f}{2\left(r_M + \dfrac{N_0}{PT_c}\right)}\right]I_0\left(\frac{\sqrt{2f}\,x_M}{r_M + \dfrac{N_0}{PT_c}}\right) \qquad \begin{array}{l} r_M = 0,1,2,\cdots \\ x_M \geq 0 \end{array} \tag{7.6}$$

where the notation of Eq. (5.3) has again been used.

For convenience, the results of Eqs. (7.2) and (7.6) may be written, respectively, as

$$p(x_k) = \frac{x_k}{\sigma_k^2}\exp\left(-\frac{x_k^2}{2\sigma_k^2}\right) \qquad x_k \geq 0 \tag{7.7}$$

where

$$\sigma_k^2 = r_k + \frac{N_0}{PT_c} \qquad \begin{array}{l} r_k = 0,1,2,\cdots \\ k = 1,2,\cdots,M-1 \end{array} \tag{7.8}$$

and

$$f(x_M) = \frac{x_M}{\sigma_M^2} \exp\left(-\frac{x_M^2 + 2f}{2\sigma_M^2}\right) I_0\left(\frac{\sqrt{2f}\,x_M}{\sigma_M^2}\right) \qquad \begin{matrix} f \geq 0 \\ x_u \geq 0 \end{matrix} \tag{7.9}$$

where

$$\sigma_M^2 = r_M + \frac{N_0}{PT_c} \qquad r_M = 0, 1, 2, \cdots \tag{7.10}$$

The probability of bit or symbol error, $\wp_e(M,1)$, for a particular set $[r_{k,j}]$ of interfering tones for the non-diversity case, i.e., N = 1, is found by substituting Eqs. (7.7) and (7.9) into Eq. (5.3) to obtain an analytical solution. The result is presented in Appendix C.

Chapter Eight

ANALYSIS OF THE DUAL-DIVERSITY CASE (N = 2)

It was shown in Chapter Six that the amplitude of the sum of r interfering tones, each of power P, and background noise of variance N_0/T_c could be approximated by a random variable drawn from the Rayleigh distribution Eq. (6.8). This was used in Chapter Seven to analyze the non-diversity case (N = 1) when using linear detectors by letting the outputs of the non-signal-bearing detectors be drawn from the Rayleigh distribution Eq. (7.7) and the output of the signal-bearing detector from the Rician distribution Eq. (7.9). It was noted that inasmuch as no diversity summations were to be performed, these also constituted the distributions of the channel outputs presented to the "largest of" selector (see Figure 4.1). Finally, it was noted that the channel selection would be the same regardless of the detector characteristic actually used, as long as it was monotone.

A closed-form solution for the symbol error probability in the non-diversity case is derived in Appendix C using the expansion given by Eq. (5.3). However, a closed-form solution does not appear to be possible for higher orders of diversity. It is shown in this chapter that a bounded solution for the symbol error probability can be obtained for the dual-diversity case (N = 2) by deriving the appropriate distributions and performing a numerical integration using the basic representation of Eq. (5.2).

For orders of diversity higher than unity, it becomes necessary, in each detection channel, to determine the distribution of the new random variable formed by summing the detector outputs over the various diversity chips. Unfortunately, the question as to which detection channel has the largest sum then depends on the type of detector that is used. To illustrate this, consider dual diversity (N = 2) in a binary FSK system (M = 2) with no noise present. Let the pair (1,7) represent the tone amplitudes present in one channel during the two diversity chips and (4,5) the tone amplitudes in the other. With a linear detector, the output of the first channel will be 1 + 7 = 8 whereas that of the second channel will be 4 + 5 = 9 leading to the selection of the second channel as the one containing the desired tone. With a square-law detector, however, the outputs will be 1 + 49 = 50 and 16 + 25 = 41 leading to the opposite conclusion. The following analysis is performed for a system using square-law detectors—the analysis when using linear detectors is analogous.

Consider first the non-signal-bearing channels in Figure 4.1. For a linear detector the output $g_{k,j}$ of the kth detector $k = 1,2,3,\cdots M-1$ at the end of the jth diversity chip is a random variable having a Rayleigh distribution of amplitudes given by Eq. (7.7) as

$$p(g_{k,j}) = \frac{g_{k,j}}{\sigma_{k,j}^2}\exp\left(-\frac{g_{k,j}^2}{2\sigma_{k,j}^2}\right) \qquad g_{k,j} \geq 0 \quad \text{Linear detector} \tag{8.1}$$

where $\sigma_{k,j}^2$ is given by Eq. (7.8) as

$$\sigma_{k,j}^2 = r_{k,j} + \frac{N_0}{PT_c} \qquad r_{k,j} = 0,1,2,\cdots \tag{8.2}$$

and where $r_{k,j}$ is the number of interfering tones present in the kth detection channel during the jth diversity chip.

It is easily shown (Papoulis, 1965) that for a square-law detector the corresponding output $g_{k,j}$ of the kth demodulator at the end of the jth diversity chip has an exponential distribution given by

$$p(g_{k,j}) = \frac{1}{2\sigma_{k,j}^2}\exp\left(-\frac{g_{k,j}}{2\sigma_{k,j}^2}\right) \qquad g_{k,j} \geq 0 \quad \text{Square law detector} \tag{8.3}$$

where $\sigma_{k,j}^2$ is again given by Eq. (8.2).

Thus, for the non-signal-bearing channels in the N = 2 case it becomes necessary to determine the distribution $p(h_{k,2})$ of

$$h_{k,2} = g_{k,1} + g_{k,2} \geq 0 \tag{8.4}$$

which is the quantity delivered to the "largest of" selector. This is done by forming the convolution

$$p(h_{k,2}) = \int_0^{h_{k,2}} p(h_{k,2} - g_{k,1})p(g_{k,2})dh_{k,2} \tag{8.5}$$

which, using Eq. (8.3), is readily integrated to yield

$$p(h_{k,2}) = \begin{cases} \dfrac{h_{k,2}}{4\sigma_k^4}\exp\left(-\dfrac{h_{k,2}}{2\sigma_k^2}\right) & \sigma_{k,1}^2 = \sigma_{k,2}^2 \equiv \sigma_k^2 \\ \dfrac{1}{2(\sigma_{k,1}^2 - \sigma_{k,2}^2}\left[\exp\left(-\dfrac{h_{k,2}}{2\sigma_{k,2}^2}\right) - \exp\left(-\dfrac{h_{k,1}}{2\sigma_{k,1}^2}\right)\right] & \sigma_{k,1}^2 \neq \sigma_{k,2}^2 \end{cases} \tag{8.6}$$

Finally, the inner integration in Eq. (5.2) can be performed yielding

$$\int_0^{x_m} p(h_{k,2})dh_{k,2} = \begin{cases} \left[1-\left(1+\dfrac{x_m}{2\sigma_k^2}\right)\exp\left(-\dfrac{x_m}{\sigma_k^2}\right)\right] & \sigma_{k,1}^2 = \sigma_{k,2}^2 \equiv \sigma_k^2 \\ \left[1-\dfrac{\sigma_{k,1}^2}{\sigma_{k,1}^2-\sigma_{k,2}^2}\exp\left(-\dfrac{x_m}{\sigma_{k,1}^2}\right)\right. & x_m \geq 0 \\ \left.-\dfrac{\sigma_{k,2}^2}{\sigma_{k,2}^2-\sigma_{k,1}^2}\exp\left(-\dfrac{x_m}{2\sigma_{k,2}^2}\right)\right] & \sigma_{k,1}^2 \neq \sigma_{k,2}^2 \end{cases} \tag{8.7}$$

(Similar results can be derived for larger values of N, but it can be seen that the number of terms involved increases rapidly.)

Consider next the Mth or signal-bearing channel in Figure 4.1. For a linear detector, the output $g_{M,j}$ of the Mth detector at the end of the jth diversity chip is a random variable having a Rician distribution of amplitudes given by Eq. (7.9) as

$$f(g_{M,j}) = \frac{g_{M,j}}{\sigma_{M,j}^2}\exp\left(-\frac{g_{M,j}^2+2f}{2\sigma_{M,j}^2}\right)I_0\left(\frac{\sqrt{2f}\,g_{M,j}}{\sigma_{M,j}^2}\right) \qquad g_{M,j} \geq 0 \quad f \geq 0 \quad \text{Linear detector} \tag{8.8}$$

where $\sigma_{M,j}^2$ is given by Eq. (7.10) as

$$\sigma_{M,j}^2 = r_{M,j} + \frac{N_0}{PT_c} \tag{8.9}$$

and where $r_{M,j}$ is the number of interfering tones in the Mth detection channel during the jth diversity chip.

It is again easily shown that for a square-law detector, the corresponding output $g_{M,j}$ of the Mth demodulator at the end of the jth diversity chip has a distribution of amplitudes given by

$$f(g_{M,j}) = \frac{1}{2\sigma_{M,j}^2}\exp\left(-\frac{g_{M,j}+2f}{2\sigma_{M,j}^2}\right)I_0\left(\frac{\sqrt{2fg_{M,j}}}{\sigma_{M,j}^2}\right) \qquad g_{M,j} \geq 0 \quad \text{Square law detector} \tag{8.10}$$

where $\sigma_{M,j}^2$ is again given by Eq. (8.9).

Thus, for the signal-bearing channel in the N = 2 case, it becomes necessary to determine the distribution $f(h_{M,2})$ of

$$h_{M,2} = g_{M,1} + g_{M,2} \geq 0 \tag{8.11}$$

which is the quantity delivered to the "largest of" selector. Unfortunately, the convolution approach used in Eq. (8.5) leads to an intractable integral when using Eq. (8.10). However, the alternative characteristic function approach is useful because it, at least, leads to a solution for the case when $g_{M,1}$ and $g_{M,2}$ are identically distributed (i.e., when the two diversity chips contain the same numbers of interfering tones). This is exemplified be Marcum and Swerling (1960) who note that the density function of the sum of independent random variables can be found by taking the inverse Fourier transform of the product of their individual characteristic functions (which are themselves Fourier transforms). In the case of Eq. (8.10), they note that matters are simplified by the fact that $f(g_{M,j})$ is defined only for non-negative values of its argument. Hence, the Laplace transform, for which extensive tabulations exist, can be used in place of the Fourier transform by simply regarding the Laplace variable p as being equivalent to the Fourier variable $i\omega$.

It is shown in Appendix D that the density function $f(h_{M,2})$, when $g_{M,1}$ and $g_{M,2}$ are identically distributed, is given by

$$f(h_{M,2}) = \frac{1}{2\sigma_M^2}\left(\frac{h_{M,2}}{4f}\right)^{1/2} \exp\left(-\frac{h_{M,2}+4f}{2\sigma_M^2}\right) I_0\left(\frac{2\sqrt{f h_{M,2}}}{\sigma_M^2}\right) \qquad \begin{array}{c} h_{M,2} \geq 0 \\ \sigma_{M,1}^2 = \sigma_{M,2}^2 \equiv \sigma_M^2 \end{array} \tag{8.12}$$

It is also shown why the result does not appear to be available in a simple form when $g_{M,1}$ and $g_{M,2}$ are not identically distributed. Nonetheless, it is possible to bound the symbol error probability in that case by using Eq. (8.12) appropriately. This can be seen by noting that if the two diversity chips contain differing numbers ($r_{M,1}$, $r_{M,2}$) of interfering tones, the symbol error probability calculated from Eq. (8.12) by assuming that both diversity chips contain the lesser of ($r_{M,1}$, $r_{M,2}$) will be less than the true symbol error probability. Similarly, the symbol error probability calculated by assuming that they both contain the greater of ($r_{M,1}$, $r_{M,2}$) will exceed the true symbol error probability.

Thus, a bound for the symbol error probability for dual-diversity operation (N = 2) can be calculated by a numerical integration of Eq. (5.2) for each set $[r_{k,j}]$ of 2M interfering tones by using the appropriate members of Eq. (8.7) for the bracketed terms used in the (M – 1)fold product and the appropriate form for $f(h_{M,2})$ from Eq. (8.12).

Chapter Nine

AN ASYMPTOTIC MODEL FOR THE HIGH-ORDER-DIVERSITY CASE (N >> 1)

A considerable simplification is possible for high orders of diversity, i.e., N >> 1, where the sums of the quadrature detector outputs, when taken over the N diversity chips, become asymptotically normal. Furthermore, the sums become identically distributed, thereby eliminating the need to consider the specific distributions of the interfering tones among the various symbol frequencies.

THE LINEAR DETECTOR

In this case, the outputs of the non-signal-bearing detectors are Rayleigh random variables and the output of the signal-bearing detector is a Rician random variable. To derive the asymptotically normal forms of the sums of these random variables, it suffices to consider only the Rician because the Rayleigh density function derives from it by setting f = 0 in Eq. (7.9). Thus, let ξ_i denote the output of the first sampler in the signal-bearing (i.e., the Mth) detection channel at the end of the ith diversity chip. Then, its probability density function is given, from Eq. (7.9), by

$$f(\xi_i) = \frac{\xi_i}{R_i} \exp\left[-\frac{\left(\xi_i^2 + 2f\right)}{2R_i}\right] I_0\left(\frac{\sqrt{2f}\,\xi_i}{R_i}\right) \qquad \xi_i, f \geq 0 \tag{9.1}$$

where

$$R_i = r_i + \frac{N_0}{PT_c} \qquad r_i = 0, 1, 2, \cdots \tag{9.2}$$

The number of interfering users r_i has a Poisson distribution given by

$$p(r) = \frac{e^{-\lambda}\lambda^2}{r!} \tag{3.9}$$

where λ, the average number of interfering users per chip, is given by Eq. (3.10). We seek the probability density function of the output x of the second sampler at the end of the Nth chip. Then,

$$x(R_1, R_2, \cdots, R_N) = \sum_{i=1}^{N} \xi_i(R_i) \tag{9.3}$$

The quantities ξ and x correspond, respectively, to $g_{m,l}$ and $h_{M,N}$ in Figure 4.1 for a linear detector.

For N large, x will be asymptotically normal $(E\,m_x, E\,\sigma_x^2)$, where m_x and σ_x^2 are the mean and variance, respectively, of x, and the expectation is necessary because x is a function of the random variables r. The first two moments of the Rician distribution are given by Rice (1945). A more convenient formulation is given by Helstrom (1968) who shows that if

$$q(\alpha, z) = z \exp\left[\frac{1}{2}(z^2 + \alpha^2)\right] I_0(\alpha z) \tag{9.4}$$

then

$$E\,z = \sqrt{\frac{\pi}{2}} \exp\left(\frac{\alpha^2}{4}\right)\left[\left(1 + \frac{\alpha^2}{2}\right) I_0\left(\frac{\alpha^2}{4}\right) + \frac{\alpha^2}{2} I_1\left(\frac{\alpha^2}{4}\right)\right] \tag{9.5}$$

and

$$E\,z^2 = 2 + \alpha^2 \tag{9.6}$$

Letting $z = \xi / \sqrt{R}$ and $\alpha^2 = 2f / R$ in Eq. (9.5) brings it into agreement with Eq. (9.1) with the result that

$$m_\xi = E\,\xi = \sqrt{\frac{\pi R}{2}} \exp\left(-\frac{f}{2R}\right)\left[\left(1 + \frac{f}{R}\right) I_0\left(\frac{f}{2R}\right) + \frac{f}{R} I_1\left(\frac{f}{2R}\right)\right] \equiv F(R, f) \tag{9.7}$$

and

$$E\,\xi^2 = 2(R + f)$$

so that

$$\sigma_\xi^2 = E\,\xi^2 - E^2\,\xi = 2(R + f) - F^2(R, f) \tag{9.8}$$

where the function F(R,f) has been introduced for simplicity in subsequent expressions.

Applying Eqs. (9.7) and (9.8) then yields

$$
\begin{aligned}
E\,m_x &= E\sum_{i=1}^{N} m_{\xi_i} = \sum_{i=1}^{N} E\,m_{\xi_i} = \sum_{i=1}^{N} E\,F(R_i, f) \\
&= \sum_{i=1}^{N} \sum_{r_i=0}^{\infty} p(r_i)F(R_i, f) = N\sum_{r=0}^{\infty} p(r)F(R, f)
\end{aligned}
\tag{9.9}
$$

Similarly,

$$
\begin{aligned}
E\,\sigma_x^2 &= E\sum_{i=1}^{N} \sigma_{\xi_i}^2 = \sum_{i=1}^{N} E\sigma_{\xi_i}^2 = \sum_{i=1}^{N} E\left[2(R_i + f) - F^2(R_i, f)\right] \\
&= \sum_{i=1}^{N} \sum_{r_i=0}^{\infty} p(r_i)\left[2\left(r_i + \frac{N_0}{PT_c} + f\right) - F^2(R_i, f)\right] \\
&= N\left[2\left(\lambda + \frac{N_0}{PT_c} + f\right) - \sum_{i=0}^{\infty} p(r)F^2(R, f)\right]
\end{aligned}
\tag{9.10}
$$

where $p(r)$ is given by Eq. (3.9) and $\sum_{r=0}^{\infty} rp(r) = \lambda$. The probability density function of x can then be written

$$
f(x) = \frac{1}{\sqrt{2\pi E\,\sigma_x^2}} \exp\left[-\frac{(x - E\,m_x)^2}{2E\,\sigma_x^2}\right]
\tag{9.11}
$$

where $E\,m_x$ and $E\,\sigma_x^2$ are given by Eqs. (9.9) and (9.10), respectively, $p(r)$ is given by Eq. (3.9), R is given by Eq. (9.2), and $F(R,f)$ is given by Eq. (9.7).

The result for the non-signal-bearing channels, in which the sampler outputs are Rayleigh, is found by setting $f = 0$ in the above results. Thus, from Eq. (9.7),

$$
F(R, 0) = \sqrt{\pi R / 2}
\tag{9.12}
$$

so Eqs. (9.9) and (9.10) become

$$
E\,m_y = \sqrt{\pi / 2}N\sum_{r=0}^{\infty} p(r)\left(r + \frac{N_0}{PT_c}\right)^{1/2}
\tag{9.13}
$$

and

$$
E\,\sigma_y^2 = N\left[2\left(\lambda + \frac{N_0}{PT_c}\right) - \sum_{r=0}^{\infty} p(r)\frac{\pi}{2}\left(r + \frac{N_0}{PT_c}\right)\right] = \left(2 - \frac{\pi}{2}\right)N\left(\lambda + \frac{N_0}{PT_c}\right)
\tag{9.14}
$$

where the variable denoting the second sampler output is written as y rather than x. Then, as in Eq. (9.11),

$$p(y) = \frac{1}{\sqrt{2\pi E\sigma_y^2}} \exp\left[-\frac{(z - Em_y)^2}{2E\sigma_y^2}\right] \tag{9.15}$$

It should be noted that p(y) applies to all of the non-signal-bearing channels, which have been made identically distributed, as well as independent, by the expectation process on r.

THE SQUARE-LAW DETECTOR

In this case, the detector characteristic to be used in Figure 4.1 is $f(\Sigma) = \Sigma$, rather than $\sqrt{\Sigma}$ as was done for the linear detector in Chapter Seven. Hence, the desired probability density function can be easily obtained by considering the square of the Rician random variable given by Eq. (9.1). Thus, the probability density function of the output of the signal-bearing channel for the square-law detector at the end of the ith chip is found to be

$$f(\xi_i) = \frac{1}{2R_i} \exp\left(-\frac{\xi_i + 2f}{2R_i}\right) I_0\left(\frac{\sqrt{2f\xi_i}}{R_i}\right) \tag{9.16}$$

where R_i is given by Eq. (9.2). We seek the probability density function of the output x of the second sampler at the end of the Nth chip. Then,

$$x(R_1, R_2, \cdots, R_N) = \sum_{i=1}^{N} \xi_i(R_i) \tag{9.17}$$

The quantities ξ and x correspond, respectively, to $g_{m,j}$ and $h_{M,N}$ in Figure 4.1 for a square-law detector.

The first two moments of ξ are readily obtained by adapting Helstrom's procedure for the Rician distribution Eq. (9.4) to the distribution for its square. Thus, if we let

$$p(\alpha, z) = \frac{1}{2} \exp\left[-\frac{1}{2}(z + \alpha^2)\right] I_0(\alpha\sqrt{z}) \tag{9.18}$$

and derive the moment-generating function, the first two moments of z are found to be

$$Ez = 2 + \alpha^2 \tag{9.19}$$

and

$$Ez^2 = 8 + 8\alpha^2 + \alpha^4 \tag{9.20}$$

which parallel Eqs. (9.5) and (9.6). These are seen to be equal to the results for the second and fourth moments given by Helstrom for the Rician distribution, which is to be expected.

To bring Eq. (9.18) into conformity with Eq. (9.16), let $z = \xi / R$ and $\alpha^2 = 2f / R$ in Eq. (9.18). Then,

$$m_\xi = E\xi = 2(R + f) \tag{9.21}$$

$$\sigma_\xi^2 = E\xi^2 - E^2\xi = 4R(R+2f) \tag{9.22}$$

Applying Eqs. (9.21) and (9.22) to Eq. (9.17) then yields

$$\begin{aligned} E\,m_x &= E\sum_{i=1}^{N} m_{\xi_i} = \sum_{i=1}^{N} E\,m_{\xi_i} = \sum_{i=1}^{N} E\,2(R_i + f) \\ &= \sum_{i=1}^{N} \sum_{r_i=0}^{\infty} p(r_i) 2\left(r_i + \frac{N_0}{PT_c} + f\right) = 2N\left(\lambda + \frac{N_0}{PT_c} + f\right) \end{aligned} \tag{9.23}$$

Similarly,

$$\begin{aligned} E\,\sigma_x^2 &= E\sum_{i=1}^{N} \sigma_{\xi_i}{}^2 = \sum_{i=1}^{N} E\,\sigma_{\xi_i}{}^2 = \sum_{i=1}^{N} E\,4R_i(R_i + 2f) \\ &= \sum_{i=1}^{N} \sum_{r_i=0}^{\infty} p(r_i) 4\left(r_i + \frac{N_0}{PT_c}\right)\left(r_i + \frac{N_0}{PT_c} + 2f\right) \\ &= 4N\left[\lambda(\lambda+1) + 2\lambda\left(\frac{N_0}{PT_c} + f\right) + \frac{N_0}{PT_c}\left(\frac{N_0}{PT_c} + 2f\right)\right] \end{aligned} \tag{9.24}$$

where

$$\sum_{r=0}^{\infty} r^2 p(r) = \lambda(\lambda + 1)$$

The probability density function of x can then be written

$$f(x) = \frac{1}{\sqrt{2\pi E\,\sigma_x^2}} \exp\left[-\frac{(x - E\,m_x)^2}{2E\,\sigma_x^2}\right] \tag{9.25}$$

where $E\,m_x$ and $E\,\sigma_x^2$ are given by Eqs. (9.23) and (9.24), respectively.

The result for the non-signal-bearing channels is found by setting f = 0 in the above results. Thus, from Eq. (9.23),

$$E\,m_y = 2N\left(\lambda + \frac{N_0}{PT_c}\right) \tag{9.26}$$

and from Eq. (9.24),

$$E\,\sigma_y^2 = 4N\left[\left(\lambda + \frac{N_0}{PT_c}\right)^2 + \lambda\right] \tag{9.27}$$

Then, as in Eq. (9.25),

$$p(y) = \frac{1}{\sqrt{2\pi E\sigma_y^2}} \exp\left[-\frac{(y - Em_y)^2}{2E\sigma_y^2}\right] \tag{9.28}$$

where $E\,m_y$ and $E\,\sigma_y^2$ are given by Eqs. (9.26) and (9.27), respectively. Again, it should be noted that p(y) applies to all of the non-signal-bearing channels, which have been made identically distributed, as well as independent, by the expectation process on r.

ANALYSIS OF THE HIGH-ORDER-DIVERSITY CASE (N >> 1)

The development in Chapter Nine led to asymptotically normal distributions for the outputs of the non-signal-bearing detection channels. This permits the formulation of the symbol error probability developed in Chapter Five using the union bound Eq. (5.7), which is applicable to conventional MFSK (with, of course, the limits of the outer integral taken over the infinite interval). Then,

$$P_e^s(M,N) \le (M-1)\int_{-\infty}^{\infty} f(x)\left[\int_{x}^{\infty} p(y)dy\right]dx \tag{10.1}$$

where f(x) and p(y) are given, respectively, by Eqs. (9.11) and (9.15) for the linear detector and by Eqs. (9.25) and (9.28) for the square-law detector. Note that Eq. (10.1) gives the actual error probability $P_e^s(M,N)$. This is because the conditioning on p(r) done in Chapter Nine is equivalent to that done in Eq. (5.8).

Though not apparent at first glance, Eq. (10.1) can be evaluated directly by suitable changes of variables, as shown in Appendix D. An ingenious alternative solution due to Gaylord Huth of RAND is presented below. It is apparent that the formulation in Eq. (10.1) calculates the probability of error as the probability that the random variable y exceeds the random variable x, where y is the amplitude of the interference in one of the non-signal-bearing detection channels and x is the amplitude of the sum of the desired tone and its accompanying interference in the signal-bearing detection channel.

Put another way, the probability of error can be taken as the probability that the random variable

$$z = y - x \tag{10.2}$$

exceeds zero. The random variable z is, of course, Gaussian with a mean

$$m_z = E\sigma_y^2 - E\sigma_x^2 \tag{10.3}$$

where Em_x and Em_y are given, respectively, by Eqs. (9.9) and (9.13) for the linear detector and by Eqs. (9.23) and (9.26) for the square-law detector and a variance

$$\sigma_z^2 = E\sigma_y^2 + E\sigma_x^2 \tag{10.4}$$

where $E\sigma_x^2$ and $E\sigma_y^2$ are given, respectively, by Eqs. (9.11) and (9.15) for the linear detector and by Eqs. (9.24) and (9.27) for the square-law detector.

Then the probability of error becomes

$$P_e^s(M,N) \le (M-1)P(z \ge 0) = (M-1)\int_0^\infty \frac{1}{\sqrt{2\pi\sigma_z^2}} \exp\left[-\frac{(z-m_z)^2}{2\sigma_z^2}\right] dz \tag{10.5}$$

A simple change of variables then yields

$$P_e^s(M,N) \le (M-1) \int_{-\frac{m_z}{\sigma_z}}^{\infty} \frac{1}{\sqrt{2\pi}} \exp\left(-\frac{t^2}{2}\right) dt = (M-1)Q\left[\frac{Em_x - Em_y}{\sqrt{E\sigma_x^2 + E\sigma_y^2}}\right] \tag{10.6}$$

which is the desired result. Here,

$$Q(x) \equiv \frac{1}{\sqrt{2\pi}} \int_x^\infty \exp(-t^2/2)\, dt \tag{10.7}$$

It should be noted from Eqs. (10.3) and (10.4) that the numerator and denominator of the Q function in Eq. (10.6) go as N and $\sqrt{N}$, respectively. Hence, the argument of the Q function goes as $\sqrt{N}$.

If, rather than using the union bound Eq. (5.7), the exact form Eq. (5.2) is used, the result is only slightly more complex than Eq. (10.6). From Eq. (5.2), considering that the non-signal-bearing detection channels are identically distributed in the asymptotic assumption, the conditional error probability becomes

$$P_e^s(M,N) = 1 - \int_{-\infty}^{\infty} f(x)\left[1 - \int_x^\infty p(y)dy\right]^{M-1} dx \tag{10.8}$$

where f(x) and p(x) are again given, respectively, by Eqs. (9.11) and (9.15) for the linear detector and by Eqs. (9.25) and (9.28) for the square-law-detector. Then, the integral on y becomes

$$\int_x^\infty p(y)dy = \int_x^\infty \frac{1}{\sqrt{2\pi E\sigma_y^2}} \exp\left[-\frac{(y-Em_y)^2}{2E\sigma_y^2}\right] dy$$

Letting

$$\frac{y - E m_y}{\sqrt{E\sigma_y^2}} = t$$

leads to

$$\int_x^{\infty} p(z)dz = \int_{\frac{x-Em_y}{\sqrt{E\sigma_y^2}}}^{\infty} \frac{1}{\sqrt{2\pi}} e^{-t^2/2} dt = Q\left(\frac{x - Em_y}{\sqrt{E\sigma_y^2}}\right)$$

Finally,

$$P_e^s(M,N) = 1 - \int_{-\infty}^{\infty} \frac{1}{\sqrt{2\pi E\sigma_x^2}} \exp\left[\frac{(x - E m_x)^2}{2E\sigma_x^2}\right]\left[1 - Q\left(\frac{(x - E m_y)}{\sqrt{E\sigma_x^2}}\right)\right]^{M-1} dx \qquad (10.9)$$

which may be used instead of Eq. (10.6).

QUADRATURE DETECTOR OUTPUT

Consider $f_k(t)$ from Eq. (4.2) as the input to the kth quadrature detector (so called because of its use of sine and cosine branches) in Figure 4.1 operating at frequency ω_k. In the cosine branch, the output of the multiplier is given by

$$\sqrt{\frac{2}{T_c}} f_k(t)\cos\omega_k t = \sqrt{\frac{2}{T_c}} \sum_{i=1}^{\rho_k} a_i \cos(\omega_i t + \theta_i)\cos\omega_k t$$

$$= \frac{1}{\sqrt{2T_c}} \sum_{i=1}^{\rho_k} a_i \left\{\cos[(\omega_i + \omega_k)t + \theta_i] + \cos[(\omega_i - \omega_k)t + \theta_i]\right\} \qquad \text{(A.1)}$$

The low-pass filter eliminates the term in $(\omega_i + \omega_k)$, so the output of the integrator is given by

$$I_{c_k} = \frac{1}{\sqrt{2T_c}} \sum_{i=1}^{\rho_k} a_i \int_0^{T_c} \cos[(\omega_i - \omega_k)t + \theta_i]dt = \sqrt{\frac{T_c}{2}} \sum_{i=1}^{\rho_k} a_i \frac{\sin x_i}{x_i} \cos(x_i + \theta_i) \qquad \text{(A.2)}$$

where

$$x_i = (\omega_i - \omega_k)T_c / 2 \qquad \text{(A.3)}$$

Similarly, the integrator output in the sine channel is given by

$$I_{s_k} = \sqrt{\frac{T_c}{2}} \sum_{i=1}^{\rho_k} a_i \frac{\sin x_i}{x_i} \sin(x_i + \theta_i) \qquad \text{(A.4)}$$

The sum of the squares of the integrator outputs becomes

$$
\begin{aligned}
\sum &= I_{c_k}^2 + I_{s_k}^2 \\
&= \frac{T_c}{2}\Bigg[\sum_{i=1}^{\rho_k} a_i^2\left(\frac{\sin x_i}{x_i}\right)^2 \cos^2(x_i+\theta_i) \\
&\quad + 2\sum_{\substack{i=1\\ i\neq j}}^{\rho_k}\sum_{j=1}^{\rho_k} a_i \frac{\sin x_i}{x_i} a_j \frac{\sin x_j}{x_j} \cos(x_i+\theta_i)\cos(x_j+\theta_j) \\
&\quad + \sum_{i=1}^{\rho_k} a_i^2\left(\frac{\sin x_i}{x_i}\right)\sin^2(x_i+\theta_i) \\
&\quad + 2\sum_{\substack{i=1\\ i\neq j}}^{\rho_k}\sum_{j=1}^{\rho_k} a_i \frac{\sin x_i}{x_i} a_j \frac{\sin x_j}{x_j} \sin(x_i+\theta_i)\sin(x_j+\theta_j)\Bigg] \\
&= \sum_{i=1}^{\rho_k} \frac{a_i^2 T_c}{2}\left(\frac{\sin x_i}{x_i}\right)^2 \\
&\quad + 2\sum_{\substack{i=1\\ i\neq j}}^{\rho_k}\sum_{j=1}^{\rho_k} \sqrt{\frac{a_i^2 T_c}{2}}\left(\frac{\sin x_i}{x_i}\right)\sqrt{\frac{a_j^2 T_c}{2}}\left(\frac{\sin x_j}{x_j}\right)\left[\cos(x_i-x_j)+(\theta_i-\theta_j)\right]
\end{aligned}
\tag{A.5}
$$

which leads to Eq. (4.3).

Appendix B

THE PROBABILITY DENSITY OF A NORMALIZED RAYLEIGH VARIABLE IN DB

We seek the probability density of the normalized interfering tone of power α_{dB} given by

$$\alpha_{dB} = 10 \log_{10} \alpha^2 \tag{6.10}$$

where the probability distribution function of α is given by

$$p_a(a) = \alpha \exp(-\alpha^2/2) \qquad \alpha \geq 0 \tag{6.7}$$

Equation (6.10) can also be written

$$\alpha = 10^{\alpha_{dB}/20} = e^{h\alpha_{dB}/20} \tag{B.1}$$

where

$$h = \log_e 10 = 2.30258\ \ 5093 \tag{B.2}$$

The probability that α_{dB} will exceed some level y is equal to the probability, from Eq. (B.1), that α will exceed $\exp(hy/20)$. Thus,

$$P(\alpha_{dB} > y) = P[\alpha > \exp(hy/20)] = \int_{\exp(hy/20)}^{\infty} p_\alpha(\alpha) d\alpha \tag{B.3}$$

The probability density function of y (which serves as surrogate for α_{dB}) then becomes

$$
\begin{aligned}
p_y(y) &= -\frac{\partial}{\partial y} P(\alpha_{dB} > y) = p_\alpha\left[\exp(hy/20)\right]\frac{d}{dy}\exp(hy/20) \\
&= \exp(hy/20)\exp\left[-\frac{\exp(hy/10)}{2}\right]\frac{h}{20}\exp(hy/20) \\
&= \frac{h}{20}\exp(hy/10)\exp\left[-\frac{1}{2}\exp(hy/10)\right] \quad -\infty < y < \infty
\end{aligned}
\tag{B.4}
$$

which leads to Eq. (6.11).

To show that $p_y(y)$ is a proper probability density function, let

$$
x = \exp(hy/10), \quad y = \frac{10}{h}\log_e x \tag{B.5}
$$

in Eq. (B.4). Then,

$$
\int_{-\infty}^{\infty} p_y(y)dy = \int_0^{\infty} \frac{h}{20} x e^{-x/2} \frac{10dx}{hx} = -e^{-x/2}\Big|_0^{\infty} = 1 \tag{B.6}
$$

as required.

To find the mean of y, use Eq. (B.4) to form

$$
\bar{y} = \int_{-\infty}^{\infty} y p_y(y)dy = \int_{-\infty}^{\infty} y \frac{h}{20}\exp(hy/10)\exp\left[-\frac{1}{2}\exp(hy/10)\right]dy \tag{B.7}
$$

Letting

$$
x = hy/10, \quad y = \frac{10}{h}x \tag{B.8}
$$

then yields

$$
\begin{aligned}
\bar{y} &= \int_{-\infty}^{\infty}\left(\frac{10}{h}x\right)\frac{h}{20}\exp x \exp\left(-\frac{1}{2}e^x\right)\frac{10}{h}dx \\
&= \frac{5}{h}\int_{-\infty}^{\infty} x e^x \exp\left(-\frac{1}{2}e^x\right)dx
\end{aligned}
\tag{B.9}
$$

From Gradshteyn and Ryzhik (1980), their Eq. 3.4811, p. 343, we have

$$\int_{-\infty}^{\infty} xe^{x}\exp(-\mu e^{x})dx = -\frac{1}{\mu}(C+\log_e \mu) \quad \mathrm{Re}\,\mu > 0 \tag{B.10}$$

where C is Euler's constant

$$C = 0.57721\ \ 56649\cdots \tag{B.11}$$

Letting $\mu = 1/2$ in Eq. (B.9) then yields

$$\bar{y} = -\frac{10}{h}\left(C + \log_e \frac{1}{2}\right) = 0.50348\ \ 41755\ \ \mathrm{dB} \tag{B.12}$$

where h is given by Eq. (B.2) and C by Eq. (B.11).

The following derivation of the second moment of y is due to William Sollfrey of RAND. From Eq. (B.4),

$$\overline{y^2} = \int_{-\infty}^{\infty} y^2 p_y(y)dy = \int_{-\infty}^{\infty} y^2\left(\frac{h}{20}\right)\exp(hy/10)\exp\left[-\frac{1}{2}\exp(hy/10)\right]dy \tag{B.13}$$

Let

$$x = \frac{1}{2}\exp(hy/10), \qquad y = \frac{10}{h}\log_e(2x) \tag{B.14}$$

Then,

$$\begin{aligned}\overline{y^2} &= \int_{0}^{\infty}\left[\frac{10}{h}\log_e(2x)\right]^2\left(\frac{h}{20}\right)2x\exp(-x)\frac{10dx}{hx} \\ &= \left(\frac{10}{h}\right)^2\int_0^{\infty}\log_e^2(2x)e^{-x}dx = \left(\frac{10}{h}\right)^2\int_0^{\infty}\left[\log_e 2 + \log_e x\right]^2 e^{-x}dx \\ &= \left(\frac{10}{h}\right)^2\int_0^{\infty}\left(\log_e^2 2 + 2\log_e 2\log_e x + \log_e^2 x\right)e^{-x}dx\end{aligned} \tag{B.15}$$

Now, consider

$$\Gamma(\alpha) = \int_0^{\infty} x^{\alpha-1}e^{-x}dx \tag{B.16}$$

Then

$$\Gamma'(\alpha) = \int_0^\infty x^{\alpha-1} \log_e x \, e^{-x} dx \tag{B.17}$$

and

$$\Gamma''(\alpha) = \int_0^\infty x^{\alpha-1} \log_e^2 x \, e^{-x} dx \tag{B.18}$$

Setting $\alpha = 1$ in Eqs. (B.16) to (B.18) and substituting in Eq. (B.15) shows that

$$\overline{y^2} = \left(\frac{10}{h}\right)^2 \left[(\log_e^2 2)\Gamma(1) + 2(\log_e 2)\Gamma'(1) + \Gamma''(1)\right] \tag{B.19}$$

To evaluate these gamma functions, consider the psi function (Abramowitz and Stegun, 1964)

$$\psi(\alpha) = \frac{d}{d\alpha} \log_e \Gamma(\alpha) = \frac{\Gamma'(\alpha)}{\Gamma(\alpha)} \tag{B.20}$$

which yields, noting that $\Gamma(1)=1$,

$$\Gamma'(1) = \psi(1) = -C \tag{B.21}$$

Also

$$\psi'(\alpha) = \frac{d^2}{d\alpha^2} \log_e \Gamma(\alpha) = \frac{\Gamma(\alpha)\Gamma''(\alpha) - [\Gamma'(\alpha)]^2}{[\Gamma(\alpha)]^2} \tag{B.22}$$

which yields

$$\psi'(1) = \Gamma''(1) - [\Gamma'(1)]^2 \tag{B.23}$$

or, using Eq. (B.21)

$$\Gamma''(1) = \psi'(1) + C^2 \tag{B.24}$$

Then, using Eqs. (B.21) and (B.24) in Eq. (B.19) yields

$$\overline{y^2} = \left(\frac{10}{h}\right)^2 \left[(\log_e 2 - C)^2 + \psi'(1)\right] \tag{B.25}$$

Finally, using Eqs. (B.25) and (B.12) leads to

$$\sigma_y^2 = \overline{y^2} - \bar{y}^2 = \left(\frac{10}{h}\right)^2 \psi'(1)$$

or, noting Eq. (B.2) and $\psi'(1) = 1.64493\ 40668$, to

$$\sigma_y = 5.57004\ \ 3140\ \ \text{dB} \tag{B.26}$$

Appendix C

DERIVATION OF THE SYMBOL ERROR PROBABILITY FOR THE NON-DIVERSITY CASE

It is desired to evaluate Eq. (5.3) for $\wp_e(M,1)$ using Eq. (7.7) for $p(x_i)$ and Eq. (7.9) for $f(x_m)$. These can be written

$$p(x_i) = \frac{x_i}{R_i} \exp\left(-\frac{x_i^2}{2R_i}\right) \tag{C.1}$$

and

$$f(x_M) = \frac{x_M}{R_M} \exp\left(-\frac{x_M^2 + 2f}{2R_M}\right) I_0\left(\frac{\sqrt{2f}\,x_M}{R_M}\right) \tag{C.2}$$

where

$$R = r + \frac{N_0}{PT_c} \tag{8.2}$$

To evaluate the general j-fold product of integrals contained in the brackets of Eq. (5.3), note that each integral has the form

$$\int_{x_M}^{\infty} p(x_k)dx_k = \int_{x_M}^{\infty} \frac{x_k}{R_k} \exp\left(-\frac{x_k^2}{2R_k}\right) dx_k = \exp\left(-\frac{x_M^2}{2R_k}\right) \tag{C.3}$$

Then, the product of j such integrals becomes

$$\Im_{R_{k_1}, R_{k_2}, \cdots, R_{k_j}} = \exp\left[-\frac{x_M^2}{2g_{R_{k_1}, R_{k_2}, \cdots, R_{k_j}}}\right] \tag{C.4}$$

where

$$\frac{1}{g_{R_{k_1},R_{k_2},\cdots R_{k_j}}} \equiv \frac{1}{R_{k_1}} + \frac{1}{R_{k_2}} + \cdots + \frac{1}{R_{k_j}} \tag{C.5}$$

The complete integrals to be summed in Eq. (5.3) can be evaluated by proper manipulation of the integrands. Thus,

$$\begin{aligned} I_{R_{k_1},R_{k_2},\cdots,R_{k_j},R_M} &= \int_0^\infty f(x_M)\Im_{R_{k_1},R_{k_2},\cdots,R_{k_j}} dx_M \\ &= \int_0^\infty \frac{x_M}{R_M} \exp\left(-\frac{x_M^2 + 2f}{2R_M}\right) I_0\left(\frac{\sqrt{2f}x_M}{R_M}\right) \exp\left[-\frac{x_M^2}{2g_{R_{k_1},R_{k_2},\cdots,R_{k_j}}}\right] dx_M \\ &= \exp\left(-\frac{f}{R_M}\right) \int_0^\infty \frac{x_M}{r_M} \exp\left[-\frac{x_M^2}{2h_{R_{k_1},R_{k_2},\cdots,R_{k_j},R_{k_M}}}\right] I_0\left(\frac{\sqrt{2f}x_M}{R_M}\right) dx_M \end{aligned} \tag{C.6}$$

where

$$\frac{1}{h_{R_{k_1},R_{k_2},\cdots,R_{k_j},R_{k_M}}} \equiv \frac{1}{R_{k_1}} + \frac{1}{R_{k_2}} + \cdots + \frac{1}{R_{k_j}} + \frac{1}{R_M} \tag{C.7}$$

To evaluate $I_{R_{k_1},R_{k_2},\cdots,R_{k_j},R_M}$, first introduce $h_{R_{k_1},R_{k_2},\cdots,R_{k_j},R_{k_M}}$ into the integrand of Eq. (C.6) in such a way that it appears in the denominator of each term. Thus,

$$\begin{aligned} I_{R_{k_1},R_{k_2},\cdots,R_{k_j},R_M} &= \frac{h_{R_{k_1},R_{k_2},\cdots,R_{k_j},R_{k_M}}}{R_M} \exp\left(-\frac{f}{R_M}\right) \\ &\int_0^\infty \frac{x_M}{h_{R_{k_1},R_{k_2},\cdots,R_{k_j},R_{k_M}}} \\ &\exp\left(-\frac{x_M^2}{2h_{R_{k_1},R_{k_2},\cdots,R_{k_j},R_{k_M}}}\right) I_0\left[\frac{\frac{h_{R_{k_1},R_{k_2},\cdots,R_{k_j},R_{k_M}}}{R_M}\sqrt{2f}x_M}{h_{R_{k_1},R_{k_2},\cdots,R_{k_j},R_{k_M}}}\right] dx_M \end{aligned} \tag{C.8}$$

Then, introduce a $\pm$ term into the argument of the exponential in such a way that it can be separated into two exponentials, of which one is not a function of x_M and the other contains a constant that is equal to half the square of the coefficient of x_M in the numerator of the Bessel function. This leads to

$$\exp\left(-\frac{x_M^2}{2h_{R_{k_1},R_{k_2},\cdots,R_{k_j},R_{k_M}}}\right)$$

$$= \exp\left[-\frac{x_M^2}{2h_{R_{k_1},R_{k_2},\cdots,R_{k_j},R_{k_M}}} \pm \frac{\left(\frac{h_{R_{k_1},R_{k_2},\cdots,R_{k_j},R_{k_M}}}{R_M}\right)^2 f}{h_{R_{k_1},R_{k_2},\cdots,R_{k_j},R_{k_M}}}\right]$$

$$= \exp\left(\frac{f\,h_{R_{k_1},R_{k_2},\cdots,R_{k_j},R_{k_M}}}{R_M^2}\right)\exp\left[-\frac{x_M^2 + \left(\frac{h_{R_{k_1},R_{k_2},\cdots,R_{k_j},R_{k_M}}}{R_M}\right)^2 2f}{2h_{R_{k_1},R_{k_2},\cdots,R_{k_j},R_{k_M}}}\right] \quad \text{(C.9)}$$

Then, Eq. (C.8) becomes

$$I_{R_{k_1},R_{k_2},\cdots,R_{k_j},R_M} = \frac{h_{R_{k_1},R_{k_2},\cdots,R_{k_j},R_{k_M}}}{R_M}\exp\left(-\frac{f}{R_M}\right)\exp\left(\frac{f\,h_{R_{k_1},R_{k_2},\cdots,R_{k_j},R_{k_M}}}{R_M^2}\right)$$

$$\int_0^\infty \frac{x_M}{h_{R_{k_1},R_{k_2},\cdots,R_{k_j},R_{k_M}}}\exp\left[-\frac{x_M^2 + \left(\frac{h_{R_{k_1},R_{k_2},\cdots,R_{k_j},R_{k_M}}}{R_M}\right)^2 2f}{2h_{R_{k_1},R_{k_2},\cdots,R_{k_j},R_{k_M}}}\right]$$

$$I_0\left(\frac{\frac{h_{R_{k_1},R_{k_2},\cdots,R_{k_j},R_{k_M}}}{R_M}\sqrt{2f}\,x_M}{h_{R_{k_1},R_{k_2},\cdots,R_{k_j},R_{k_M}}}\right)dx_M \quad \text{(C.10)}$$

A comparison of the integrand in Eq. (C.10) with the probability density function of $f(x_m)$ in Eq. (7.9) shows that it, too, is a probability density function. Hence, its integral equals unity and Eq. (C.10) can be written

$$I_{R_{k_1},R_{k_2},\cdots,R_{k_j},R_M} = \frac{h_{R_{k_1},R_{k_2},\cdots,R_{k_j},R_{k_M}}}{R_M}\exp\left[-\frac{f}{R_M}\left(1-\frac{h_{R_{k_1},R_{k_2},\cdots,R_{k_j},R_{k_M}}}{R_M}\right)\right] \quad \text{(C.11)}$$

where $h_{R_{k_1},R_{k_2},\cdots,R_{k_j},R_{k_M}}$ is given by Eq. (C.7). Finally, substituting Eq. (C.11) in Eq. (5.3) yields

$$\wp_e^s(M,1) = \sum_{k_1=1}^{M-1} I_{R_{k_1},R_M} - \sum_{\substack{k_1=1 \\ k_1\neq k_2}}^{M-1} \sum_{k_2=1}^{M-1} I_{R_{k_1},R_{k_2},R_M} + \cdots$$
$$-(-1)^{M-1} \sum_{k_1=1}^{M-1} \sum_{\substack{k_2=1 \\ k_1\neq k_2\neq\cdots\neq k_{M-1}}}^{M-1} \cdots \sum_{k_M=1}^{M-1} I_{R_{k_1},R_{k_2},\cdots,R_{k_{M-1}},R_M} \tag{C.12}$$

which is the desired result.

DERIVATION OF THE DENSITY FUNCTION OF THE SUM OF THE SQUARES OF TWO IDENTICALLY DISTRIBUTED INDEPENDENT RICIAN RANDOM VARIABLES

Consider the squares of two identically distributed independent Rician random variables. Their density functions, from Eq. (8.10), are given by

$$f_1(x) = f_2(x) = \frac{1}{2\sigma^2}\exp\left(-\frac{x+2f}{2\sigma^2}\right) I_0\left(\frac{\sqrt{2fx}}{\sigma^2}\right) \qquad x \geq 0 \tag{D.1}$$

To simplify the analysis let $t = x/2\sigma^2$. Then,

$$f_1(t) = f_2(t) = \left|2\sigma^2\right| f(2\sigma^2 t) = \exp\left(-t - \frac{f}{\sigma^2}\right) I_0\left(2\sqrt{\frac{ft}{\sigma^2}}\right) \qquad t \geq 0 \tag{D.2}$$

From Erdelyi et al.(1954), using the notation

$$g(p) = \int_0^\infty \epsilon^{-pt} f(t)\, dt \tag{D.3}$$

it is seen that their Eq. 4.16(14) gives the Laplace pair

$$f(t) = I_0\left(2\sqrt{at}\right) \qquad g(p) = \frac{1}{p} e^{a/p} \tag{D.4}$$

and their Eq. 4.1(5) gives the Laplace pair

$$e^{-bt} f(t) \qquad g(p+b) \tag{D.5}$$

Hence, the desired Laplace pair, obtained by multiplying both by c, is

$$ce^{-bt} I_0\left(2\sqrt{at}\right) \qquad \frac{c}{p+b}\exp\left(\frac{a}{p+b}\right) \tag{D.6}$$

which agrees with Eq. (D.2) when

$$a=\frac{f}{\sigma^2} \qquad b=1 \qquad c=e^{-a}=e^{-f/\sigma^2} \tag{D.7}$$

For the sum of the two random variables given by Eq. (D.2), the Laplace transform to be inverted is the square of the right-hand member of Eq. (D.6) or

$$g(p)=\frac{c^2}{(p+b)^2}\exp\left(\frac{2a}{p+b}\right) \tag{D.8}$$

To find the inverse transform of Eq. (D.8) consider the Laplace pair given by Erdelyi et al. (1954), Eq. 5.5(36),

$$\frac{1}{p^{\upsilon+1}}\exp\left(\frac{2a}{p}\right) \qquad \left(\frac{t}{2a}\right)^{\upsilon/2} I_\upsilon\left(\sqrt{2at}\right) \tag{D.9}$$

Then, by using Eq. (D.4), letting $\upsilon=1$, and multiplying both terms by c, these become

$$\frac{c^2}{(p+b)^2}\exp\left(\frac{2a}{p+b}\right) \qquad c^2e^{-bt}\left(\frac{t}{2a}\right)^{1/2} I_1\left(2\sqrt{2at}\right) \tag{D.10}$$

The left-hand member of Eq. (D.10) now agrees with Eq. (D.8) so the desired inverse transform is given by the right-hand member. Substituting for a, b, and c from Eq. (D.7) then yields

$$\begin{aligned} f(t)&=e^{-2f/\sigma^2}e^{-t}\left(\frac{t}{2f/\sigma^2}\right)^{1/2} I_1\left(2\sqrt{\frac{2ft}{\sigma^2}}\right) \\ &=\left(\frac{\sigma^2 t}{2f}\right)^{1/2}\exp\left(-t-\frac{2t}{\sigma^2}\right) I_1\left(2\sqrt{\frac{2ft}{\sigma^2}}\right) \end{aligned} \tag{D.11}$$

Making the change of variables $x = 2\sigma^2 t$ then leads to

$$\begin{aligned} f(x)&=\frac{1}{|2\sigma^2|}f\left(\frac{x}{2\sigma^2}\right)=\frac{1}{2\sigma^2}\left(\frac{\sigma^2 x/2\sigma^2}{\sigma f}\right)^{1/2}\exp\left(-\frac{x}{2\sigma^2}-\frac{2f}{\sigma^2}\right) I_1\left(2\sqrt{\frac{2fx/2\sigma^2}{\sigma^2}}\right) \\ &=\frac{1}{2\sigma^2}\left(\frac{x}{4f}\right)^{1/2}\exp\left(-\frac{x+4f}{2\sigma^2}\right) I_1\left(\frac{2\sqrt{fx}}{\sigma^2}\right) \qquad x\geq 0 \end{aligned} \tag{D.12}$$

which is the desired result appearing as Eq. (8.12). It is equivalent to the Marcum and Swerling (1960) result, Eq. (37), for N = 2.

It may be noted that if $\sigma^2 \neq \sigma^2$, then $f_1(x)$ and $f_2(x)$ in Eq. (D.1) will have different parameters σ_1^2 and σ_2^2. Hence, it is not possible to make the initial change of variables that led to the simpler forms $f_1(t)$ and $f_2(t)$ in Eq. (D.2). Instead, it becomes necessary to deal directly with $f_1(x)$ and $f_2(x)$ whose Laplace transforms yield the product, analogous to Eq. (D.8), given by

$$g(p) = g_1(p)g_2(p) = \frac{c_1 c_2}{(p+b_1)(p+b_2)} \exp\left(\frac{a_1}{p+b_1} + \frac{a_2}{p+b_2}\right) \tag{D.13}$$

where

$$a = \frac{f}{2\sigma^4} \qquad b = \frac{1}{2\sigma^2} \qquad c = \frac{1}{2\sigma^2} e^{-f/\sigma^2} \tag{D.14}$$

with suitable subscripts. The author was unable to find the inverse Laplace transform of Eq. (D.13).

DERIVATION OF THE SYMBOL ERROR PROBABILITY FOR THE HIGH-ORDER-DIVERSITY CASE

When Eqs. (9.11) and (9.15) are substituted in Eq. (10.1), the symbol error probability takes the form

$$P_e^s(M,N) \le (M-1)\int_{-\infty}^{\infty} \frac{1}{\sqrt{2\pi E\,\sigma_x^2}} \exp\left[-\frac{(x-E\,m_x)^2}{2E\,\sigma_x^2}\right] \left\{\int_x^{\infty} \frac{1}{\sqrt{2\pi E\,\sigma_x^2}} \exp\left[-\frac{(z-E\,m_z)^2}{2E\,\sigma_z^2}\,dz\right]\right\} dx \tag{E.1}$$

Let $(x - E\,m_x)/\sqrt{E\,\sigma_x^2} = u$ in the outer integral. Then,

$$P_e^s(M,N) \le (M-1)\int_{-\infty}^{\infty} \frac{1}{\sqrt{2\pi}} \exp\left(-\frac{u^2}{2}\right) \left\{\int_{\sqrt{E\sigma_x^2}\,u+E\,m_x}^{\infty} \frac{1}{\sqrt{2\pi E\,\sigma_z^2}} \exp\left[-\frac{(z-E\,m_z)^2}{2E\,\sigma_z^2}\right] dz\right\} du \tag{E.2}$$

Next, let $(z - E\,m_z)/\sqrt{E\,\sigma_z^2} = v$ in the inner integral. Then,

$$P_e^s(M,N) \le (M-1)\int_{-\infty}^{\infty} \frac{1}{\sqrt{2\pi}} \exp\left(-\frac{u^2}{2}\right) \left\{\int_{au+b}^{\infty} \frac{1}{\sqrt{2\pi}} \exp\left[-\frac{v^2}{2}\right] dv\right\} du \tag{E.3}$$

where

$$a = \frac{\sqrt{E\,\sigma_x^2}}{\sqrt{E\,\sigma_z^2}} \quad b = \frac{E\,m_x - E\,m_z}{\sqrt{E\,\sigma_z^2}} \tag{E.4}$$

The region of integration of Eq. (E.3) in the $u - v$ plane is shown in Figure E.1a as the shaded region, the boundary of which is a distance

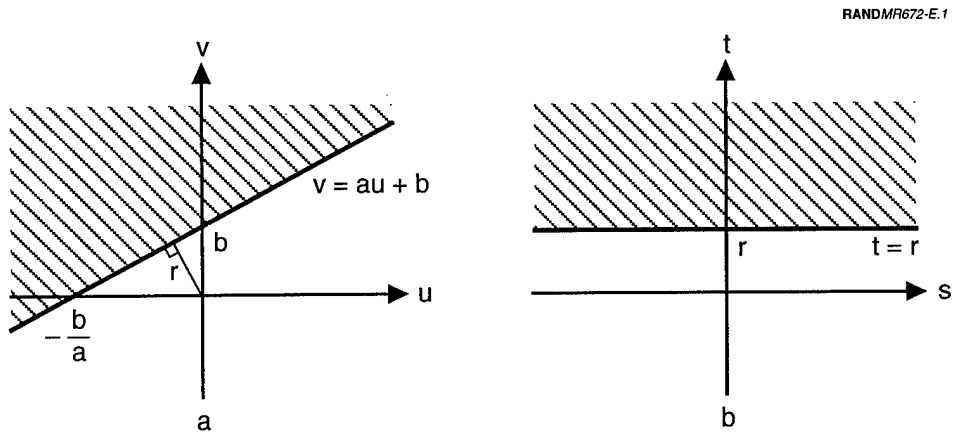

Figure E.1—Regions of Integration for Symbol Error Probability in the High-Order-Diversity Case

$$r = \frac{b}{\sqrt{1+a^2}} = \frac{E\,m_x - E\,m_z}{\sqrt{E\,\sigma_x^2 + E\,\sigma_z^2}} \tag{E.5}$$

from the origin. Inasmuch as p(u) and p(v) in Eq. (E.3) are independent, zero mean, unit variance, Gaussian distributions, it follows from symmetry that the region of integration can be rotated about the origin as indicated in Figure E.1b. It immediately follows that Eq. (E.3) can be written

$$\begin{aligned} P_e^s(M,N) &\le (M-1)\int_{-\infty}^{\infty}\frac{1}{\sqrt{2\pi}}\exp\left(-\frac{s^2}{2}\right)ds\int_{r}^{\infty}\frac{1}{\sqrt{2\pi}}\exp\left(-\frac{t^2}{2}\right)dt \\ &= (M-1)Q(r) = (M-1)Q\left[\frac{E\,m_x - E\,m_z}{\sqrt{E\,\sigma_x^2 + E\,\sigma_z^2}}\right] \end{aligned} \tag{10.6}$$

where

$$Q(x) \equiv \frac{1}{\sqrt{2\pi}}\int_{x}^{\infty}\exp\left(-\frac{t^2}{2}\right)dt \tag{E.6}$$

REFERENCES

Abramowitz, M., and I. A. Stegun, *Handbook of Mathematical Functions with Formulas, Graphs, and Mathematical Tables,* Applied Mathematics Series 55, National Bureau of Standards, Washington, D.C., June 1964.

Cramér, H., *Mathematical Methods of Statistics,* Princeton University Press, Princeton, New Jersey, 1946.

Dwight, H. B., *Tables of Integrals and Other Mathematical Data,* revised edition, MacMillan Publishing Company, New York, 1947.

Erdelyi, A., W. Magnus, F. Oberhettinger, and F. G. Tricomi, *Tables of Integral Transforms,* Vol. 1, McGraw-Hill Book Company, New York, 1954.

Fenton, L. F., "The Sum of Log-Normal Probability Distributions in Scatter Transmission Systems," *Trans. IEEE,* Vol. CS-8, No. 1, March 1960, pp. 57–67.

French, R. C., "The Effect of Fading and Shadowing on Channel Reuse in Mobile Radio," *Trans. IEEE,* Vol. VT-28, August 1979, pp. 171–181.

Gradshteyn, I. S., and I. M. Ryzhik, *Tables of Integrals, Series, and Products,* corrected and enlarged edition prepared by Alan Jeffrey, Academic Press, New York, 1980.

Helstrom, C. W., *Statistical Theory of Signal Detection,* second edition, Pergamon Press, New York, 1968.

Loo, C., "Digital Transmission Through a Land Mobile Satellite Channel," *Trans. IEEE,* Vol. COM-38, No. 5, May 1990, pp. 693–697.

Marcum, J. I., *A Statistical Theory of Target Detection by Pulsed Radar,* RAND, RM-754, Santa Monica, California, December 1, 1947.

Marcum, J. I., *A Statistical Theory of Target Detection by Pulsed Radar: Mathematical Appendix,* RAND, RM-753, Santa Monica, California, July 1, 1948.

Marcum, J. I., and P. Swerling, "Studies of Target Detection by Pulsed Radar," *Trans. IRE,* Vol. IT-6, No. 2, April 1960.

Papoulis, A., *Probability, Random Variables, and Stochastic Processes,* McGraw-Hill Book Company, New York, 1965.

Rice, S. O., "Mathematical Analysis of Random Noise," *Bell System Technical Journal*, Vol. 23, No. 3, July 1944, pp. 282–332; Vol. 24, No. 1, January 1945, pp. 46–156.

Simon, M. K., J. K. Omura, R. A. Scholtz, and B. K. Levitt, *Spread Spectrum Communications*, Computer Sciences Press, Rockville, Maryland, 1985.

Sklar, B., *Digital Communications Fundamentals and Applications*, Prentice Hall, Englewood Cliffs, New Jersey, 1988.

Stiffler, J. J., *Theory of Synchronous Communications*, Prentice-Hall, Englewood Cliffs, New Jersey, 1971.

Swerling, P., *Probability of Detection for Fluctuating Targets*, RAND, RM-1217, Santa Monica, California, March 17, 1954.

Viterbi, A. J., *Principles of Coherent Communication*, McGraw-Hill Book Company, New York, 1966.

Viterbi, A. J., "The Orthogonal-Random Waveform Dichotomy for Digital Mobile Personal Communication," *IEEE Personal Communications*, Vol. 1, No. 1, First Quarter 1994, pp. 18–24.

Ziemer, R. E., and R. L. Peterson, *Digital Communications and Spread Spectrum Systems*, MacMillan Publishing Company, New York, 1985.